

AFDELINGEN FOR
BÆRENDE KONSTRUKTIONER
DANMARKS TEKNISKE HØJSKOLE



STRUCTURAL RESEARCH LABORATORY
TECHNICAL UNIVERSITY OF DENMARK

Arne Ryden Egerup, H. J. Larsen, H. Riberholt
and Erik Sørensen

PAPERS PRESENTED AT
IUFRO - V,
INTERNATIONAL UNION OF FORESTRY
RESEARCH ORGANIZATION,
DIVISION V,
CONGRESS 1973

RAPPORT NR. R 52 1974

Papers presented at
IUFRO - V
International Union of Forestry Research Organization
Division V
Congress 1973

Arne Ryden Egerup:	
Ultimate load of timber trusses determined by the limit analysis method	1 - 15
H.J. Larsen:	
The yield load of bolted and nailed joints	16 - 31
H.J. Larsen & Erik Sørensen:	
Joints with conical steel pins	32 - 53
H.J. Larsen:	
Structural failures in Denmark 1971-73	54 - 55
H.J. Larsen & H. Riberholt:	
Note on determination of characteristic values	56 - 61
Nordic Building Regulations Committee:	
Code for specification of strength and stiffness values for wood based boards	62 - 71

Figure 1



ULTIMATE LOAD OF TIMBER TRUSSES
DETERMINED BY THE LIMIT ANALYSIS METHOD

Arne Ryden Egerup
B.Sc. M.Sc.

Structural Research Laboratory
Technical University of Denmark

Synopsis.

Design of timber trusses according to the linear theory of elasticity is known to be conservative. A more advanced computerized analysis reproduces the deformation pattern quite accurately, but gives only a poor indication of the ultimate load.

Ultimate load is usually determined by full-scale testing. This can be expensive, particularly if a series of tests is undertaken to develop a family of truss designs.

This report presents a method based on the plastic limit analysis theory to determine the ultimate load. The analysis takes advantage of the ability of the material to redistribute stresses beyond the elastic limit, and offers an analytical estimation of the factor of safety.

A comparison between the ultimate loads obtained from actual tests on a number of different W-trusses and those predicted by the outlined procedure verify the theory taking the complexity of the structure into account.

Introduction.

Prefabricated timber roof trusses are widely used in small building construction. Today the prefabricated timber trusses are taking over most of the market due to their suitability for industrial mass production.

Considering the number of units every year ($\frac{1}{2}$ mill. in Denmark) it is especially important from an economic point of view that the design give an optimum structure fulfilling the functional requirements during the service time.

The functional requirements are specified in the building codes and vary from country to country, but the main requirements will be that the structure has sufficient stiffness to keep the deflection below a given permissible value, and must be strong enough to carry the expected loads with a certain factor of safety.

It is common practice, in order to get a new truss design accepted, to predict the performance either by full-scale prototype testing or structural analysis, or by a combination of more advanced analytical procedures with performance tests.

The methods of structural analysis are normally entirely based on the elastic theory, mainly using the stiffness method on a mathematical model of the real structure⁵. This structural analog may be as simple or as complex as necessary to produce a complete structural analysis by using a computerized system. The deformation pattern of the structure is reproduced quite accurately by this procedure, hence the acceptability of the service-load deformations is sufficiently checked, but the procedure does only give an indication of the ultimate load of the structure.

Design methods which are entirely based on the elastic limit fail to take advantage of the ability of some components in redundant structures to redistribute stresses beyond the

elastic limit. These redistributed stresses can often carry very considerable additional loads. Therefore, from this viewpoint, elastic analysis is unduly conservative.

The object of the research described in this report was to develop a method based on the plastic limit analysis which would give a reasonably realistic estimate of the factor of safety for timber trusses. The plastic analysis combined with the elastic analysis would then ensure an appropriate design with respect to factor of safety and performance for working load. It must be pointed out that the outlined procedure does not pay any attention to the stability of the members,² long-term load⁷, local damage, fatigue and vibration which may govern particular designs. These must be introduced into the design separately.

Derivation of Theoretical Relationship.

The behaviour of a timber truss when the applied load is increased to failure of the truss is illustrated by a load-deflection curve in fig. 1.

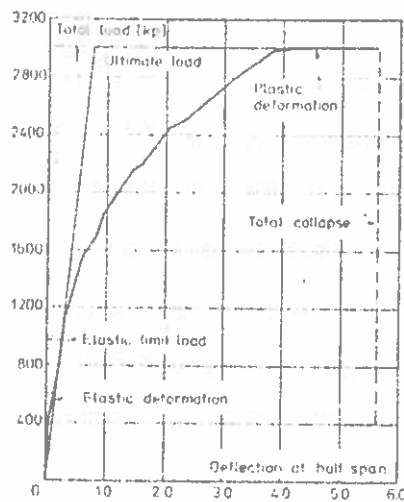


Fig. 1. Typical load deflection curve for a W-truss, with plywood plates nailed to spruce.

For loads beyond the elastic limit local regions of the truss will be plastic and the stresses will exceed the elastic limit stresses. This ductility in redundant structures permits a

redistribution of stresses beyond the elastic limit and enables the structure to carry further increased loads until total collapse or local fracture.

Properties of the components.

Member characteristics.

Wood is normally regarded as a linear elastic material. However, while wood in tension and compression has almost perfect elastic behaviour this is not the case with wood in bending. Fig. 2 shows a uniaxial stress strain diagram for wood

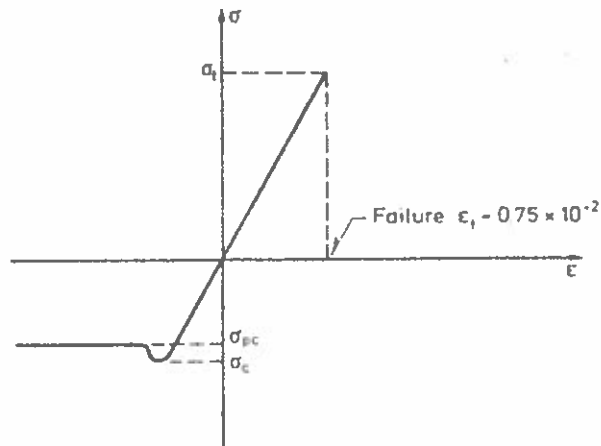


Fig. 2. Stress strain diagram for wood.

The curve is linear respectively to the tensile stress σ_t and the compression stress σ_{pc} . Failure in tension occurs by rupture of the fibres, while failure in compression occurs by folding of the fibres, but without any total collapse of the compression fibres. The stress of the fibres in compression will, after the folding process, decrease to approximately 2/3 of the maximum value (ultimate compressive stress). For combined bending and axial stresses the moment capacity will remain nearly constant, when the fibres in compression have reached the ultimate compressive stress.

Fig. 3 shows the bending capacity of a timber beam with depth h as a function of the curvature.

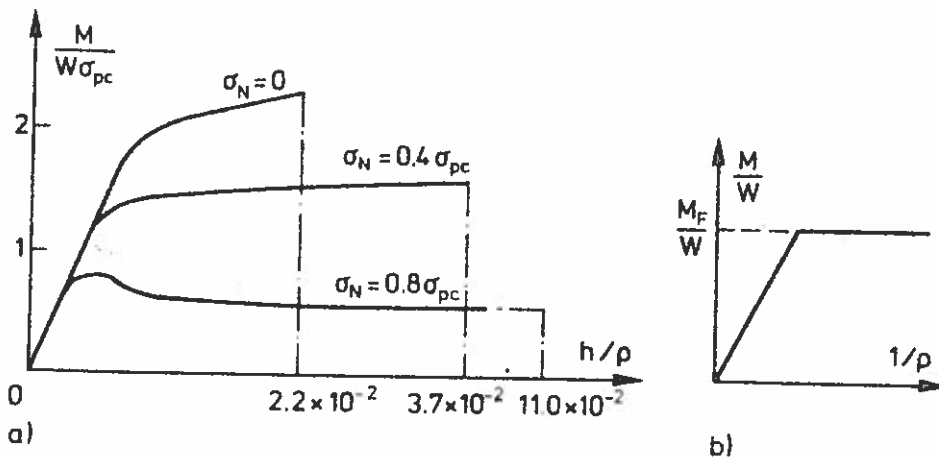


Fig. 3 Diagram of moment versus curvature for a rectangular cross section.

It can be seen from the plots that the bending capacity is dependent on the axial force, but as shown in Fig. 3.b the curves from Fig. 3.a can be idealized by a perfect elastic plastic function where M_F is the maximum plastic moment (yield moment).

There is only a limited amount of information about bending capacity available in the existing literature. Due to lack of information the relationship between the plastic moment and plastic force was evaluated assuming an idealized stress distribution as shown in Fig. 4.

Fig. 5 gives a dimensionless graph of the function between the plastic moment and the axial yield force for a rectangular cross section which can be expressed by

$$\frac{M_F}{M_{OF}} = \left(1 + n \frac{N_F}{N_{OF}}\right) \left(1 - \frac{4n}{3n-1} \frac{N_F}{N_{OF}}\right) \quad (1)$$

where M_{OF} is the plastic moment for no axial force and N_{OF} is the plastic force for no moment.

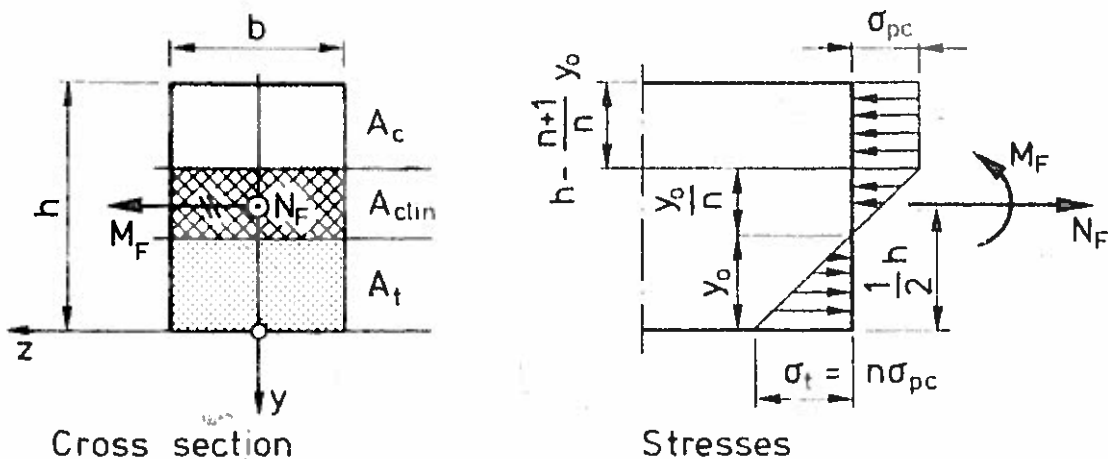


Fig. 4 Idealized stress distribution for combined bending and tension.

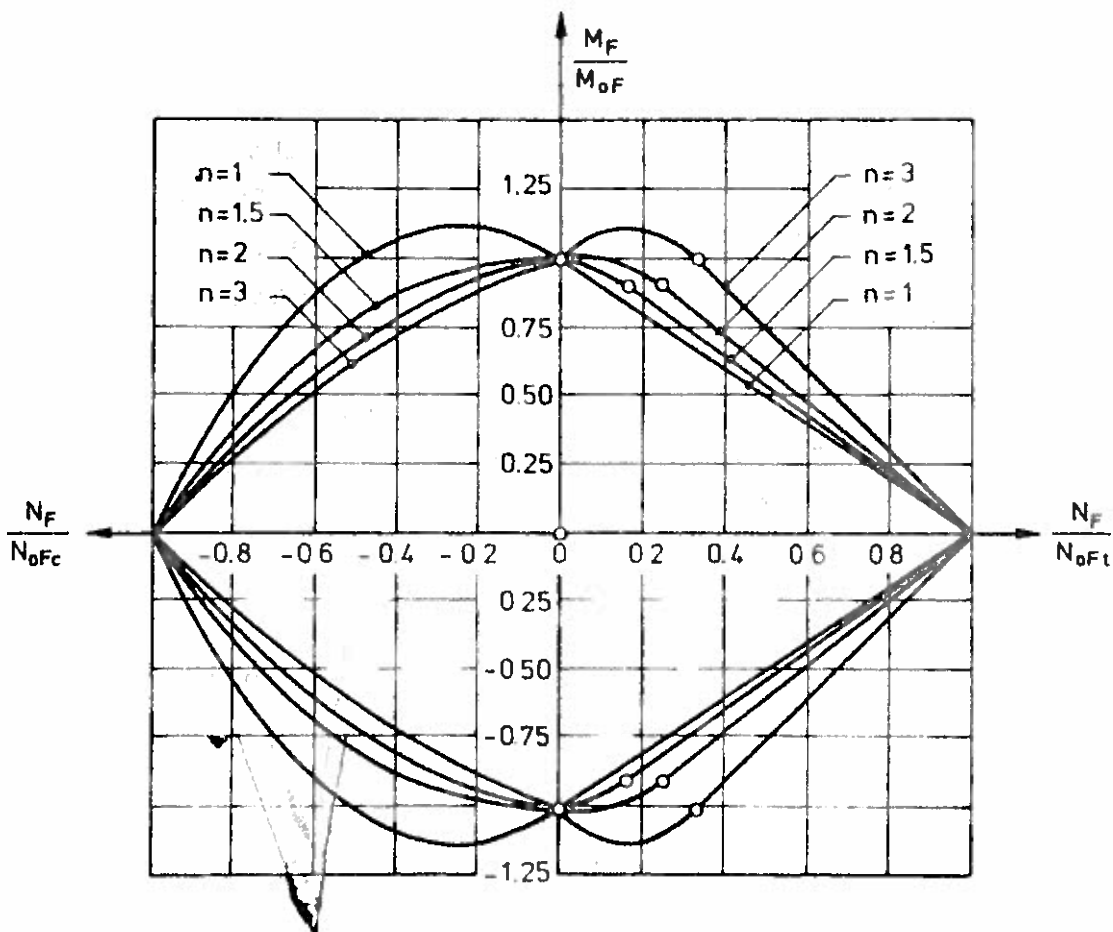


Fig. 5 Dimensionless graph of plastic moment versus plastic force.

Joint characteristics.

The joint characteristics are given by the load slip diagram for a specific fastener. Fig. 6 shows a

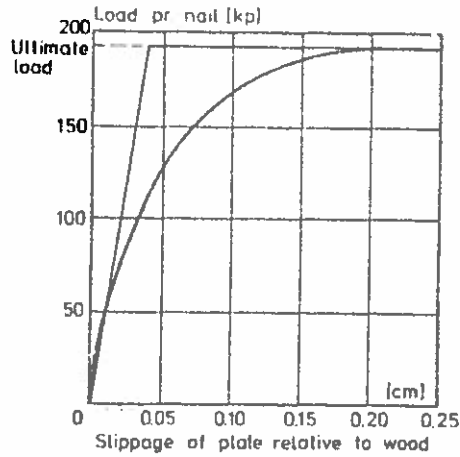


Fig. 6 Load slip diagram of light gauge toothed plates in spruce.

typical load slip diagram. For most types of fasteners the curve can be idealized by a perfect elastic plastic function, where S_F is the maximum yield force. The yield force can be determined by a simple loading arrangement with specimens in tension.

Method of limit analysis.

The complete solution to a plastic analysis problem involves finding a field which is both statically and kinematically admissible¹⁾. The limit analysis theorems lead to an upper bound in the case of a kinematically admissible field, whereas a statically admissible field produces a lower bound. The actual collapse load can therefore be obtained by considering all possible upper bounds and selecting the lowest one.

By means of the principle of virtual work the actual collapse load P for a mechanism can be determined by the equation (2) which expresses the internal work to the external work.

$$\sum M_F \cdot \theta + \sum S_F \cdot s = \int F(x) W^* (x) dx \quad (2)$$

The left hand side is the internal work done by the plastic moment on the rotations θ in the hinges and the yield force on the elongation of connection in the yield points. The right hand side is the work done by the external forces F on the virtual displacements W^* .

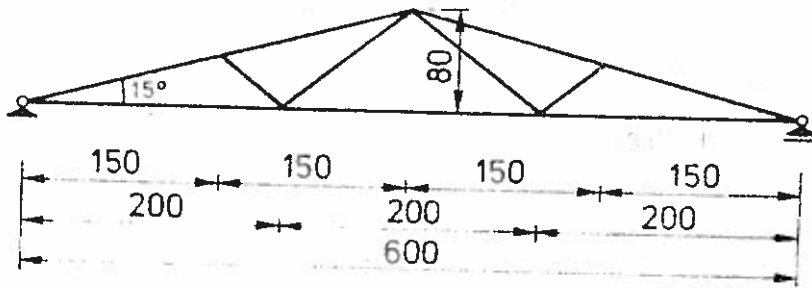
For a complex structure this principle becomes very elaborate, but for the simple W truss only a few collapse mechanisms are possible.

However, for more complex structures a computer program based on linear elastic-perfect plastic analysis was used to search for the collapse mechanism giving the lower bound.

Fig. 7 and fig. 8 show the possibilities for a W truss with loads applied respectively at the joints and between the joints. The formulas given for the ultimate load for the different mechanisms are determined from the actual geometry of the trusses used for the experimental verification (page 10).

All other combinations are easily determined by superposition of the elementary mechanisms.

An alternative method to the principle of virtual work is the method of inequalities, which reverses the procedure and finds the largest possible lower bound.



Truss geometry [cm]

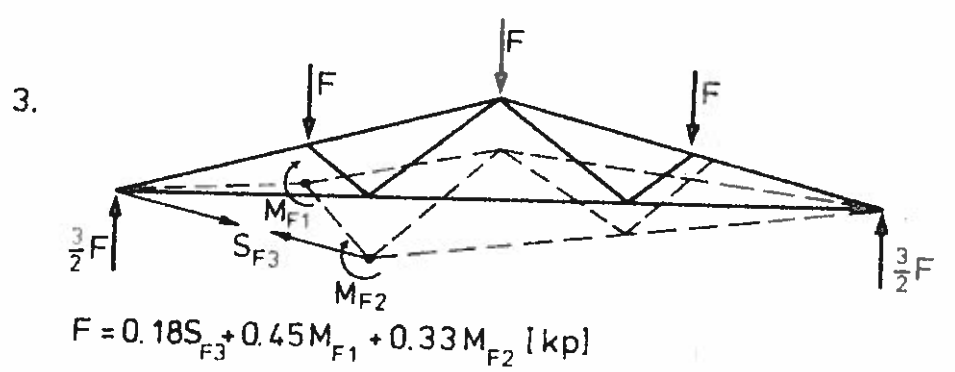
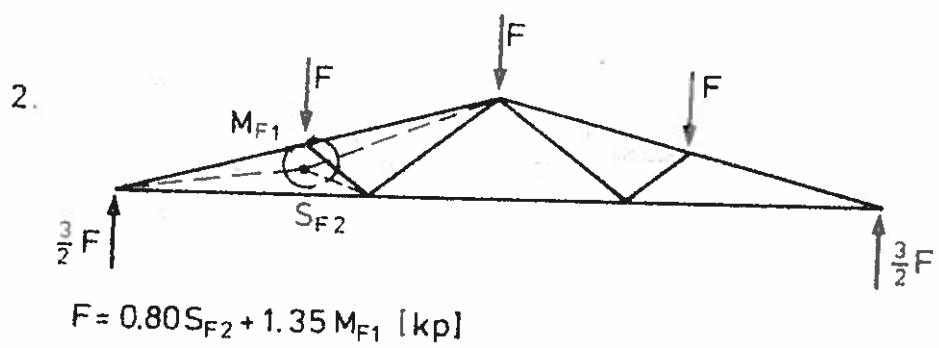
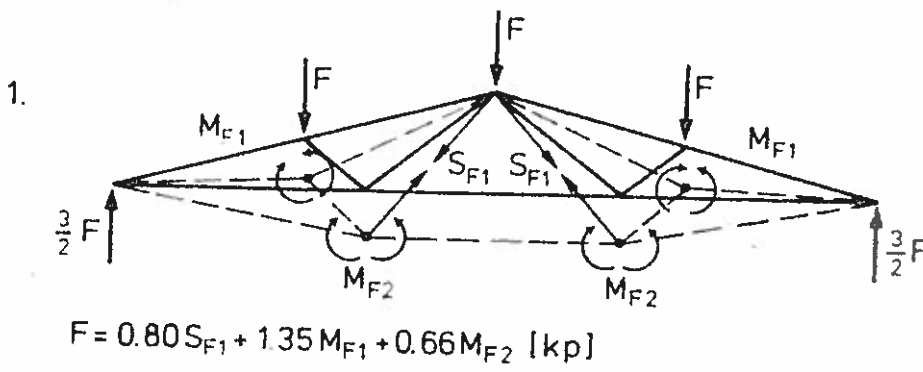


Fig. 7. Collapse mechanisms for loadcase A.

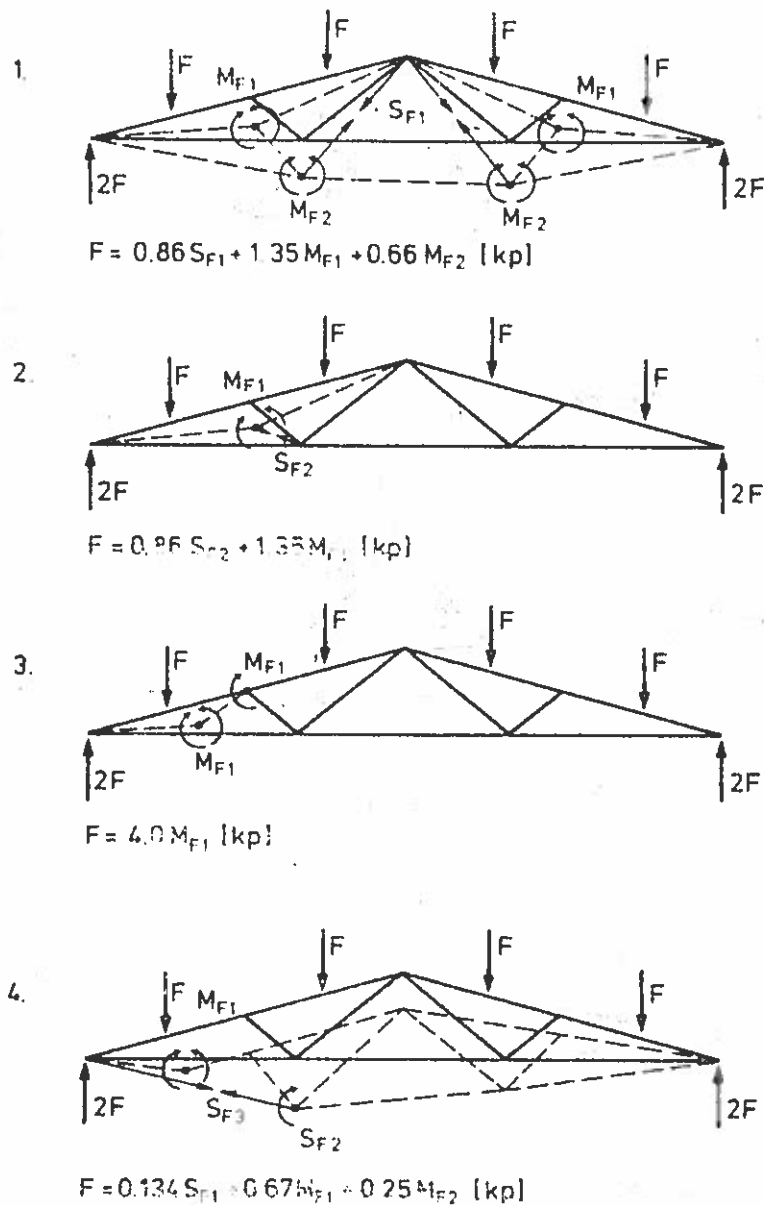


Fig. 8. Collapse mechanisms for loadcase B.

The techniques described so far are concerned with finding the theoretical load-carrying capacity of a structure made of an ideal plastic material. However, there will be various limitations for applicability of these ideal solutions to the real physical problems.

It is necessary to pay attention to the local deformations. The idealization of a yield hinge concentrated at one point of a beam implies that the strain at the outer fibres of the beam

is going to infinity. In practice, the hinge is spread over a finite portion of the beam, and only finite strains result. However, these strains may be sizeable and if they are too large, a local fracture may ensue. Therefore the displacements of the structure must be considered to ensure that failure occurs as a collapse mechanism, and not as a local fracture in which case the ultimate load may be considerably less than that produced by the limit analysis. For complex structures a computer program based on linear elastic-perfect plastic analysis will check for local fracture and produce the corresponding load.

Experimental verification.

Experimental research was carried out to verify the theoretical predicted ultimate load of the W-truss and the actual behaviour of the truss under both elastic and plastic conditions.

Descriptions of the specimens.

Trusses with a roof slope of 15° and a span of 6 m but with different member sizes of the upper and lower chord and different joint characteristics were produced. In the joints were used 2.5 mm metal-plate connectors with 20/40 mm nails. The trusses were made of spruce commercial grade (50 grade), (No. 2 grade).

Description of Loading apparatus.

In a test rig the loads were applied to the laterally supported truss with hydraulic jacks and the loads recorded by a pressure cell in the hydraulic system. The deflections were measured for each load-step using dial gauges.

Loading Procedure and Results.

In order to obtain the linear portion of the load deflection curve the load was precycled once and then applied stepwise with a magnitude of 1/10 of the expected ultimate load. This

is necessary in order to set the joint connectors in the wood foundation. The structures in service are subjected to a similar condition.

As well as the truss experiments proper, secondary tests were carried out in order to establish the quality of the material used, as expressed by its modulus of elasticity, ultimate compressive strength, humidity etc.

Two types of loading condition were used: loads applied at the joint (load case A) and loads applied at the mid-point of the upper chord members (load case B).

The results are summarized in Tables 1 and 2. Comparisons of experimental and theoretical results are shown in Fig. 9 as a plot of experimental versus theoretical results. The coefficient of correlation is 0.71 and the highest deviation approximately 23%.

In general, the theory predicted the ultimate load very well. Variation between experimental and theoretical values was expected due to the variation within the components of the trusses.

The results were considered to be an acceptable verification of the theory taking the complexity of the structures and material into account.

Truss No.	Top chord size nom.	Bottom chord size nom.	Number of Nails in			Ultimate Load F Theory [kp]	Ultimate Load F Test [kp]
			Heel point	Short diagon.	Long diagon.		
1.1	2x7	2x4	2x22	2x5	2x10	1430	1420
2.1	-	-	-	-	2x8	-	1610
3.1	-	-	-	-	2x6	-	1360
4.1	2x7	2x5	2x28	2x5	2x12	1710	1880
5.1	-	-	-	-	2x10	-	1460
6.1	-	-	-	-	2x8	-	1815
7.1	2x6	2x4	2x22	2x5	2x10	1310	1530
7.2	-	-	-	-	2x10	-	1290
8.1	-	-	-	-	2x8	-	1660
9.1	-	-	-	-	2x6	-	1300
10.1	2x6	2x5	2x28	2x5	2x12	1600	1630
11.1	-	-	-	-	2x10	-	1560
11.2	-	-	-	-	2x10	-	1420
12.1	-	-	-	-	2x8	-	1480
13.1	2x5	2x4	2x22	2x5	2x10	1200	1460
14.2	-	-	-	-	2x8	-	1500
14.2	-	-	-	-	2x8	-	1170
15.1	-	-	-	-	2x6	-	1400
16.1	2x5	2x5	2x28	2x5	2x12	1490	1680
16.2	-	-	-	-	2x12	-	1500
17.2	-	-	-	-	2x10	-	1500
18.2	-	-	-	-	2x8	-	1780
19.1	2x4	2x4	2x22	2x5	2x10	1115	1360
19.2	-	-	-	-	2x10	-	1240
20.1	-	-	-	-	2x8	-	1180
20.2	-	-	-	-	2x8	-	1190
21.1	-	-	-	-	2x6	-	950
21.2	-	-	-	-	2x6	-	1040
22.1	2x4	2x5	2x28	2x5	2x12	1405	1520

Table 1. Summary of truss details and theoretical and experimental results for loadcase A.

Truss No.	Top chord size nom.	Bottom chord size nom.	Number of Nails in			Ultimate Load F ^T Theory [kp]	Ultimate Load F ^T Test [kp]
			Heel point	Short diagon.	Long diagon.		
3.0	2x7	2x4	2x22	2x5	2x6	1385	1590
4.0	2x7	2x5	2x28	-	2x12	1565	1205
5.0	-	-	-	-	2x10	-	1625
6.0	-	-	-	-	2x8	-	1435
7.0	2x6	2x4	2x22	-	2x10	1205	1290
9.0	-	-	-	-	2x6	-	995
10.0	2x6	2x5	2x28	-	2x12	1390	1305
12.0	-	-	-	-	2x8	-	1250
13.0	2x5	2x4	2x22	-	2x10	1040	1365
14.0	-	-	-	-	2x8	-	1115
15.0	-	-	-	-	2x6	-	990
17.0	2x5	2x5	2x28	-	2x10	1250	1220
18.0	-	-	-	-	2x8	-	1085
22.0	2x4	2x5	-	-	2x12	1130	1280

Table 2. Summary of truss details and theoretical and experimental results for loadcase B.

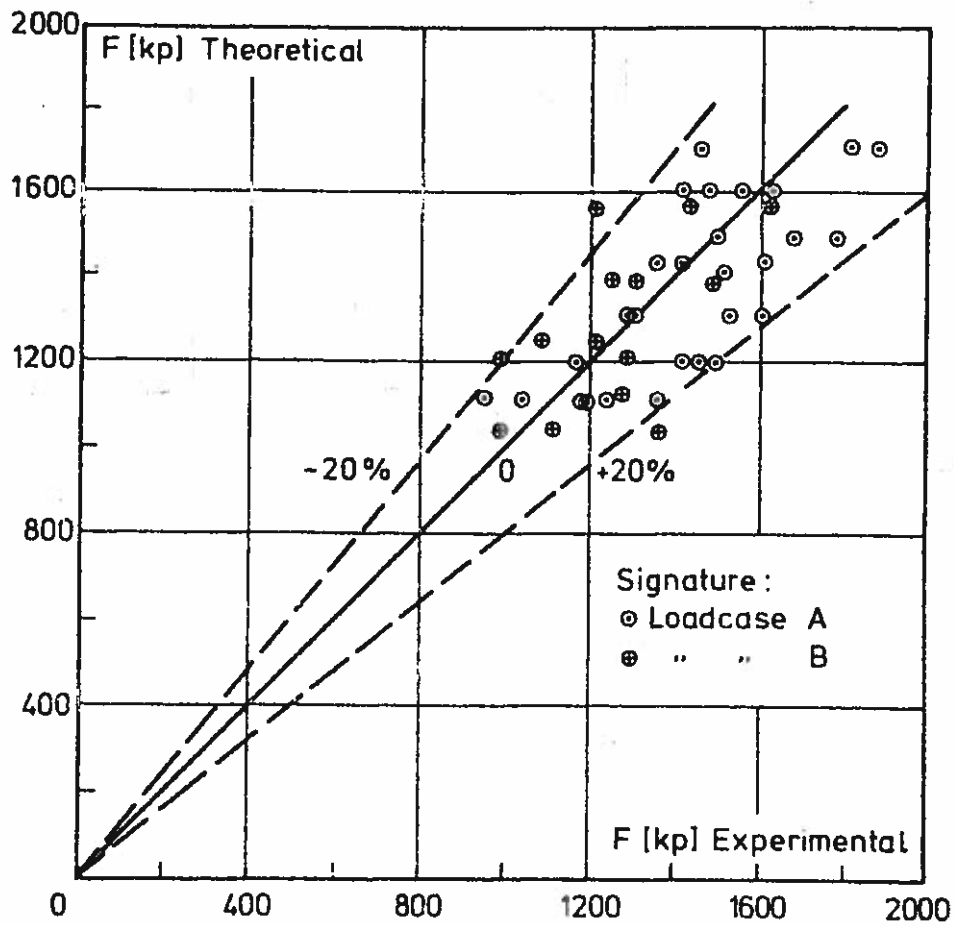


Fig. 9. Plot of experimental values versus theoretical values.

Conclusion.

Plastic limit analysis is not an alternative method to the elastic analysis, but must be considered as an additional method which enables the designer to give a realistic estimation of the factor of safety. An acceptable design of a structure requires analysis of the performance both under elastic and plastic conditions.

Plastic limit analysis is mathematically simple and can easily be applied in advanced computerized optimum design procedures for development of new structures.

References.

- [1] Brynildsen, O.A. and Booth, L.G.
Structural Analysis of Timber Trusses with semi-rigid Joints. Imperial College, London (1967).
- [2] Egerup, A.R. Lateral stability of two- and three-hinged glulam arches. University of British Columbia, Vancouver (1972).
- [3] Hansen, A.T. Deflections of wooden roof trusses based on simple joint tests. Research paper no. 334. National Research Council of Canada (1967).
- [4] Hodge, P.G. Plastic Analysis of Structures. Illinois Institute of Technology. McGraw-Hill (1959).
- [5] Reardon, G.F. A Structural Analysis of Frames with semi-rigid joints. Division of Forest Products. Paper no. 59 CSIRO, Melbourne (1961).
- [6] Suddarth, S.K. A Computerized Wood Engineering System - The Purdue Plane Structure Analyzer, U.S. Forest Products Laboratory, FPL 168, Madison, Wisconsin (1972).
- [7] Wilkinson, T.L. Longtime Performance of Trussed Rafters: Initial evaluation, Forest Products Laboratory, Forest Service, U.S. Department of Agriculture (1958).

THE YIELD LOAD OF BOLTED AND NAILED JOINTS

H.J. Larsen

Structural Research Laboratory
Technical University of Denmark.

SYNOPSIS

An account is given of a theoretical determination of the bearing capacity (yield strength, ultimate strength) of dowels, bolts, nails and similar, based on the assumption that the stress-strain curve for bending of the dowel and for embedment of the dowel corresponds to a stiff-plastic material. Expressions for the bearing capacity of arbitrary single and double shear joints are derived. The expressions are as an example applied to joints with bolts and nails in ordinary structural timber (Nordic spruce or fir), and simple, approximate expressions are given for bolts.

INTRODUCTION

In the Nordic countries the bearing capacity of dowels, bolts, nails and similar is fixed on the basis of the ultimate bearing capacity (yield strength). Tests have shown that this can be determined theoretically on the basis of knowledge of the prism strength of the wood and the yield moment of the bolt. In the following general expressions are first formulated for use in, for example, the calculation of joints between wood and plywood or steel and concrete, after which they are specialized corresponding to joints in Nordic structural timber. The basis was first given in generally applicable form by K.W. Johansen [1].

THEORY

Material assumptions.

Fig. 01 shows the stress-strain diagram in bending for mild steel. θ is a measure of the bending deformation, while M is the bending moment.

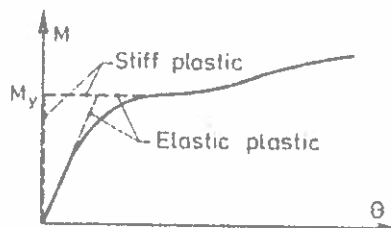


Fig. 01.

The real stress-strain curve is frequently approximated by assuming either that the material is perfectly elastic-perfectly plastic or, more simply, that it is stiff-plastic. In the following, the latter approximation will be used. The yield moment can be written as

$$M_y = W_p \sigma_y \quad (01)$$

where W_p is the plastic moment of resistance and σ_y is the tensile yield stress (strength) of the steel. For a circular cross-section

[1] Johansen, K.W.: Theory of Timber Connections. International Association for Bridge and Structural Engineering. Publications. Vol. 9, 1949.

$$W_p = d^3/6 \tag{02}$$

where d is the diameter.

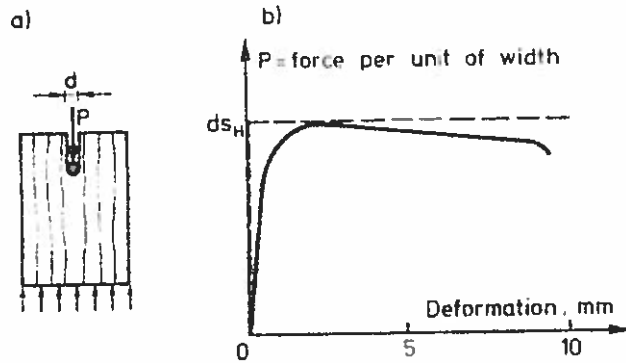


Fig. 02.

In embedding tests with a dowel in wood as shown in fig. 02a, a stress-strain curve as shown in fig. 02b is obtained. At the beginning there is a linear relationship between force and embedment, while at the end a "plastic" state occurs, with a long, almost horizontal stress-strain curve.

Along the horizontal part of the curve, the load per unit length of the dowel is written as ds_H , where d is the diameter of the dowel and s_H is the mean stress under the dowel, i.e. the stress resulting from considering, as a rough simplification, that the pressure is uniformly distributed. s_H is called the embedding strength and depends on a large number of factors, principally the prism strength of the wood s_p , but also the cross-sectional shape and diameter of the dowel, and the angle v between the direction of the force and that of the fibres.

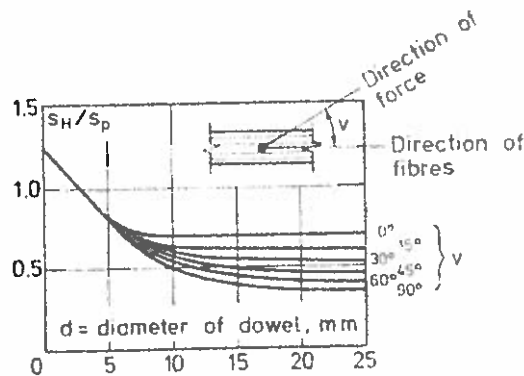


Fig. 03.

The variation in the ratio s_{Hv}/s_p with the direction of the force and the dowel diameter is by tests found to be as shown in fig. 03. The values in the figure, for the force acting parallel to and at right-angles to the fibres, are calculated on the basis of the bearing capacity of tested dowel joints. For intermediate values of the angle v , we interpolate in accordance with the formula,

$$s_{Hv} = s_{H0} - (s_{H0} - s_{H90})\sin v. \quad (03)$$

In embedding tests, e.g. as shown in fig. 02, slightly different values are found for the ratio s_H/s_p .

In the following the bearing capacity of dowel joints will be determined on the basis of the approximation that the stress-strain curve for the dowel and its embedment in the wood is stiff-plastic. The bearing capacity can also be determined on slightly less rigorous assumptions, see e.g. [2], but for practical purposes, the simple theory gives completely satisfactory results, inter alia because, as indicated in connexion with fig. 03, it entails an adjustment of the material constants.

Built-in dowel.

Let us first consider a simple case: a circular dowel of diameter d placed in a piece of wood with thickness l and loaded by a force P_y at a distance e from one side of the piece of wood, see fig. 04.

Case 1.

It is first assumed that the dowel is so stiff that it only gets negligible elastic deformations. The dowel may then rotate about a point at a distance x from one side, see fig. 04a. As it is assumed that the stress-strain curve for embedment is stiff-plastic, the load on the dowel will be

[2] Larsen, H.J. and Vagn Reestrup: Tests on Screws in Wood. Bygningsstatistiske Meddelelser, Vol. 40, No. 1, 1969.

as shown in b, and the internal forces as shown in c and d.

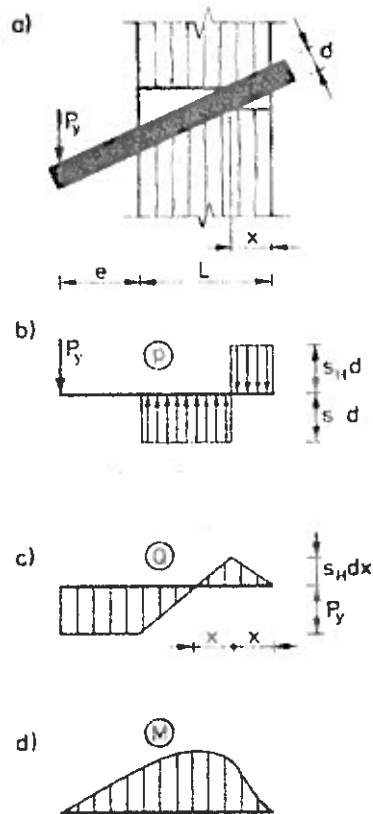


Fig. 04.

By projection, we find

$$P_y = (L - 2x)s_H d \quad (04)$$

and by moment about the force

$$s_H d \left[x \left(L - \frac{x}{2} + e \right) - (L - x) \left(\frac{L-x}{2} + e \right) \right] = 0$$

Hence

$$x = L + e - \frac{1}{2} \sqrt{(L + 2e)^2 + L^2}$$

and

$$P_y = (\sqrt{(L + 2e)^2 + L^2} - (L + 2e))s_H d \quad (05)$$

The maximum moment is then

$$M_{\max} = x^2 s_H d$$

and (05) applies as long as $M_{\max} \leq M_y$.

Case 2.

If $M_{\max} \geq M_y$, conditions will be as shown in fig. 05.

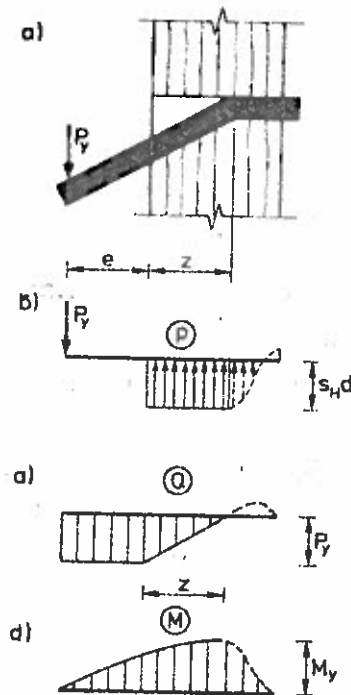


Fig. 05.

The yield moment of the dowel is reached at a point at a distance z from the surface. With the idealized stress-strain curve, the dowel will at this point bend sharply and otherwise

remain straight. Over the length z , the pressure from the wood will be $s_H d$, while the pressure is otherwise indeterminate but less than $s_H d$. If the friction forces on the surface of the dowel can be neglected, Q will be zero at the point of deflection as the moment here has its maximum value M_y , and by vertical projection and moment about the point of deflection, we find

$$P_y = z s_H d$$

and

$$M_y = P_y \left(e + z - \frac{z}{2} \right)$$

Hence

$$z = \sqrt{e^2 + \frac{2M_y}{s_H d}} - e \quad (06)$$

and

$$P_y = \left(\sqrt{e^2 + \frac{2M_y}{s_H d}} - e \right) s_H d \quad (07)$$

Single shear joints.

We will now examine an arbitrary single shear joint that has to transmit a force located at a distance y from one of the joint surfaces. We wish to find the maximum value P_y of the force.

One of the pieces of wood has the thickness $L_1 = l$, and the embedding strength $s_{H1} = s_H$, while the other has the thickness $L_2 = \alpha L$ and the embedding strength $s_{H2} = \beta s_H$, see fig. 06.

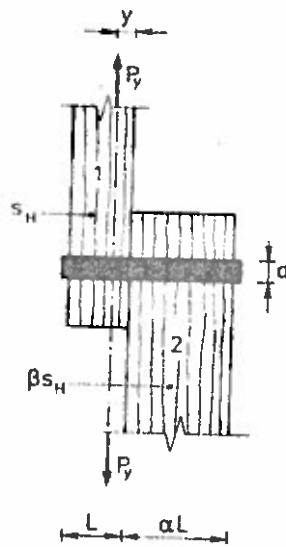


Fig. 06.

For this case four different types of rupture are possible. These are shown in fig. 07.

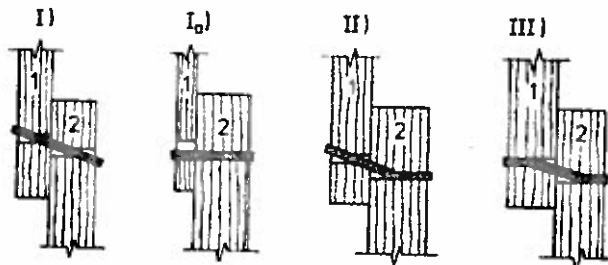


Fig. 07.

In rupture type I, the diameter d of the dowel is so thick that the dowel remains straight during rupture. Thus, in both pieces of wood, conditions correspond to the case denoted 1 in the previous section. If one of the pieces of wood is much thicker than the other, rotation will be prevented and rupture will then be of type Ia, where the dowel is subject to parallel displacement in the weakest piece of wood.

Rupture types II and III occur if the loads on the dowel become so big prior to development of rupture type I that the yield moment is reached at one or two points. If the dowel only yields at one point, rupture pattern II will occur, while III corresponds to yielding of the dowel in both pieces of wood.

For rupture types I, II and III, the bearing capacity can be found by requiring that rupture occur simultaneously in both pieces.

For rupture type I in piece 1, we find from (05), with $e = -y$:

$$P_y = (\sqrt{(L - 2y)^2 + L^2} - (L - 2y))s_H d \quad (08)$$

and in piece 2, from (05), with $e = +y$:

$$P_y = (\sqrt{(\alpha L + 2y)^2 + (\alpha L)^2} - (\alpha L + 2y))\beta s_H d \quad (09)$$

Eliminating y from these expressions, we get

$$I: P_y = Lds_H \frac{\sqrt{\beta + 2\beta^2 + 2\alpha\beta^2 + 2\alpha^2\beta^2 + \alpha^2\beta^3} - \beta(1 + \alpha)}{1 + \beta} \quad (10)$$

However, P_y cannot exceed

$$Ia: P_y = Ls_H d \text{ for } \alpha\beta \geq 1 \quad (11)$$

or

$$Ia: P_y = \alpha\beta Ls_H d \text{ for } \alpha\beta \leq 1 \quad (12)$$

corresponding to rupture type Ia.

For rupture type II, (08) still applies in piece 1, but in piece 2 we find from (07):

$$P_y = (\sqrt{y^2 + \frac{2M_y}{\beta s_H d}} - y)\beta s_H d \quad (13)$$

Eliminating y , we get

$$II: P_y = s_H d L \frac{\beta}{2 + \beta} \left[\sqrt{\frac{2(1 + \beta)}{\beta} + \frac{4(2 + \beta)}{\beta} \cdot \frac{M_y}{s_H d L^2}} - 1 \right] \quad (14)$$

In the derivation it is assumed that the yield point of the dowel lay in piece 2. If yielding occurs in the other piece, we find by inversion:

$$\text{II: } P_y = s_H d L \frac{\sigma \beta}{2\beta + 1} \left[\sqrt{2(1 + \beta) + \frac{4(1 + 2\beta)}{\beta} \cdot \frac{M_y}{s_H d \alpha^2 L^2}} - 1 \right] \quad (15)$$

For rupture type III in piece 1, we find from (07):

$$P_y = \left(\sqrt{(-y)^2 + \frac{2M_y}{s_H d}} + y \right) s_H d$$

while (13) applies in piece 2.

Eliminating y , we get

$$\text{III: } P_y = \sqrt{4M_y s_H d \frac{\beta}{1 + \beta}} \quad (16)$$

The expression, (10) - (12) and (14) - (16) that gives the lowest value of P_y is valid.

From the basic expression given above, we can also determine the location of the force in the joint (the quantity y). If the external load did not originally correspond to this, the structure will seek to deform in order to achieve correspondence. As an example, is in fig. 0.8 shown the simple lapped joint.



Fig. 08.

Double shear joints.

Only symmetrical double shear joints will be examined. Asymmetrical joints are rather rare in practice, and the inaccuracy arising in calculating an asymmetrical joint as a symmetrical joint with the thickness of both side pieces equal to the thinnest side piece in the connexion is insignificant. The

thickness of the side pieces is $L_1 = L$, while that of the middle piece is $L_2 = \alpha L$. The side pieces have the embedding strength $s_{H1} = s_H$, while the middle piece has $s_{H2} = \beta s_H$.

Rupture can occur in four different ways in this joint, see fig. 09.

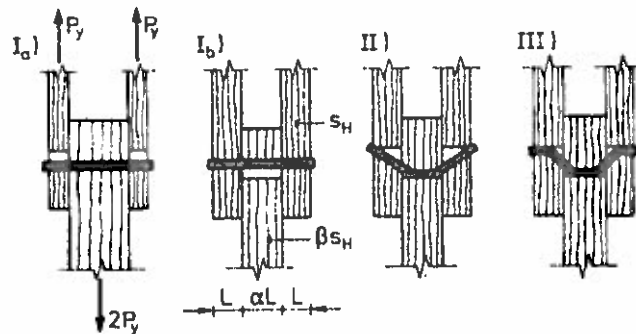


Fig. 09.

If the dowel is stiff, rupture will occur in the form of crushing, either in the side pieces (Ia) or in the middle piece (Ib).

If the dowel is insufficiently stiff it will yield, either in the middle piece (rupture type II) or both in the side and the middle pieces (rupture type III). A state with yielding only in the side pieces is not possible.

Denoting the bearing capacity per shear plane P_y , we find for rupture type Ia:

$$\text{Ia: } P_y = Lds_H \text{ for } \alpha\beta \geq 2 \quad (17)$$

and for rupture type Ib,

$$\text{Ib: } P_y = \frac{1}{2}\alpha\beta Lds_H \text{ for } \alpha\beta \leq 2 \quad (18)$$

For rupture types II and III, it will be seen that P_y is the same as for the corresponding types of rupture in single shear.

The special case $\beta = 1$.

The expressions found are rather complicated, due particularly to the factor β . Expressions will, therefore, first be given for the special case, $\beta = 1$, which corresponds to the common case in which pieces of wood with the same fibre direction are to be joined.

In single shear joints we find for $\beta = 1$:

$$I: P_y = \frac{1}{3}Lds_H[\sqrt{3 + 2\alpha + 3\alpha^2} - (1 + \alpha)] \quad (19)$$

$$Ia: P_y = Lds_H \quad (20)$$

$$II: P_y = \frac{1}{3}Lds_H\left(\sqrt{4 + \frac{12M_y}{s_H d L^2}} - 1\right) \quad (21)$$

$$III: P_y = \sqrt{2M_y s_H d} \quad (22)$$

It is assumed that $\alpha \geq 1$. The results are shown in fig. 10 for $\sigma_y/s_H = 10$, which corresponds to the value for s_H found for Nordic timber and ordinary bolts, see below:

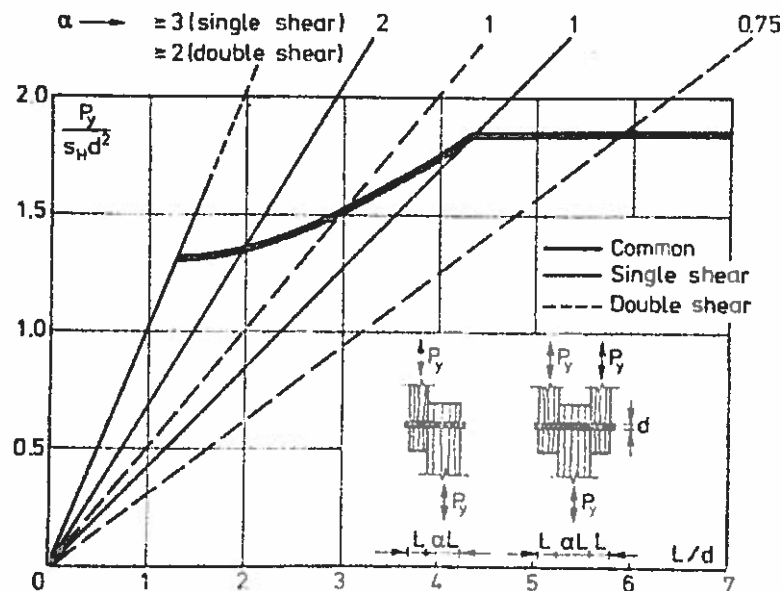


Fig. 10.

For double shear joints, (19) and (20) are substituted by (17) and (18), with $\beta = 1$.

The special case $\beta = 0.5$.

For thick dowels, we find, cf. fig. 03, that s_H for loading perpendicular to the fibres is about half the value for loading parallel to the fibres. Therefore, for single joints in which one piece of wood is perpendicular to the other, we have $\beta = 0.5$, while in double joints in which the middle piece is perpendicular to the side pieces, we have $\beta = 0.5$ or $\beta = 2.0$, depending on the direction of the force, cf. fig. 11, where the bearing capacity for double shear joints of this type is shown in relationship to the ratio L/d for the same ratio between σ_y and s_H as above.

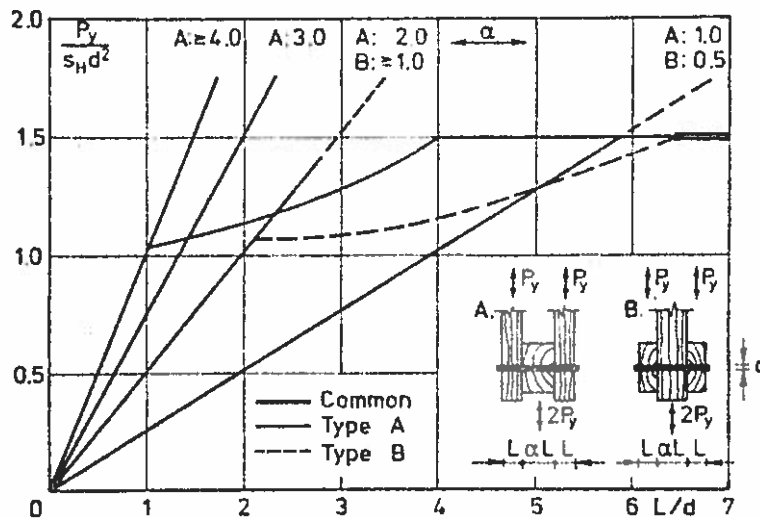


Fig. 11.

BOLTS AND NAILS

Bolts.

Structural timber from the Nordic countries, with a moisture content of under about 20% and for short-term loading, can be taken to have a prism strength of 35 N/mm^2 (characteristic value corresponding to the 5% fractile). The corresponding embedding strengths are shown in fig. 03.

For ordinary bolts (quality D40), it can be reckoned that $\sigma_y = 240 \text{ N/mm}^2$.

The characteristic ultimate bearing capacities can then be found from the expressions derived in the foregoing after adding to the material parameters the necessary safety factors (poss. partial coefficients), reductions for long-term loading, etc.

The expressions are rather complicated. The Danish Code of Practice for Timber constructions [3] therefore specifies approximate expressions, which, without safety factor, are as follows:

For single shear joints:

$$P_y = \min \begin{cases} 6.1(k_1 L_1 + k_2 L_2) d \\ 24.5 k_1 L_1 d \\ 4.3 k_1 L_1 d + 24 d^2 \\ 44 d^2 \sqrt{\frac{k_1 + k_2}{2}} \sqrt{\frac{\sigma_F}{240}} \end{cases} \quad (23)$$

[3] Danish Standard DS 413.

For double shear joints:

$$P_y = \min \begin{cases} 12.3 k_2 L_2 d \\ 24.5 k_1 L_1 d \\ 4.3 k_1 L_1 d + 24 d^2 \\ 44 d^2 \sqrt{\frac{k_1 + k_2}{2}} \sqrt{\frac{\sigma_F}{240}} \end{cases} \quad (24)$$

Here,

d diameter of the dowel in mm.

L_1 thickness in mm of thinnest piece of wood in single shear joints or of side pieces in double shear joints.

L_2 thickness in mm of thickest piece of wood in single shear joints or of middle piece in double shear joints.

k_1 and k_2 factors obtained from the following table 12 and taking into account the angle between the direction of the force and that of the fibres in the pieces of wood with thickness L_1 and L_2 . The table is just another way of presenting fig. 03.

Table 12.

Angle between direction of force and direction of fibres	k for bolt diameter (in mm)					
	≤ 6	10	12	16	20	25
0°	1	1	1	1	1	1
30°	1	0,92	0,89	0,86	0,82	0,80
45°	1	0,84	0,80	0,75	0,70	0,67
60°	1	0,78	0,72	0,67	0,61	0,57
90°	1	0,73	0,66	0,59	0,54	0,50

The values in (23) and (24) are characteristic values for short-term loads.

For permanent loading, the values are according to [3] reduced by the factor 0.60 (corresponding to the British 9/16). In

certain cases this is conservative (in the bottom line of (23) and (24), the reduction is only $\sqrt{0.6}$), but it is chosen in order to obtain simple rules since for short-term loading it is then always possible to increase the values by the same factors as used for wood.

Nails.

The nails commonly used in Denmark are drawn wire nails with full square cross-section.

According to tests, they have a yield moment,

$$M_y = \sigma_y W_p = 45(20-a) \frac{a^3}{4} \text{ Nmm} \quad (25)$$

and the characteristic short-term value of the embedding strength, see fig. 0.3, is as follows, with a prism strength of 35 N/mm^2 :

$$s_H = 0.09 \cdot (14-a) \cdot 35 \text{ N/mm}^2 \quad (26)$$

a is the edge length of the nails in mm.

Because of splitting, nails are always chosen sufficiently long to achieve rupture type III, and the characteristic short-term bearing

$$P_y = \sqrt{2 \cdot 11.25 \cdot (20-a) \cdot a^3 \cdot 0.09(14-a) \cdot 35 \cdot a} \\ = 8.4 \cdot a^2 \cdot \sqrt{(20-a)(14-a)} \quad (27)$$

Here, too, the long-term strength is in [3] set conservatively at 60% of the short-term strength.

JOINTS WITH CONICAL STEEL PINS

H.J. Larsen

Erik Sørensen

Structural Research Laboratory
Technical University of Denmark.

This project was partly financed by a grant to Erik Sørensen from TOP (The Timber Promotion Organization).

INTRODUCTION

In timber structures, joints are often executed with nailed steel gussets. Compared with wooden or plywood gussets, steel gussets mean that the joint can be made thinner, the risk of splitting is reduced, and the bearing capacity of the nails is increased.

In light structures, such thin gussets are often used that it is possible to nail through them without pre-drilling. Because of the danger of buckling, the gussets are frequently placed between the wooden parts.

For heavier loads thicker gussets are used, and in this case it is necessary to drill the holes in advance. This means that a number of the advantages are lost because the holes often have to be drilled a little too big, at any rate for the square nails normally used in Denmark.

In order to avoid these drawbacks, a special nail (the glulam rivet) has been developed for this purpose in Canada [1a] and [1b], with the head shaped so that it rivets itself into the gusset.

Such a special nail is hardly warranted for a small market like Denmark, and a substitute has therefore been sought. It has been found that conical steel pins, as used in the engineering industry, are suitable.

Basically, the joints are as shown in fig. 1.

In the following an account is given of the theoretical bearing capacity and stiffness. This is followed by a description of tests carried out, which partly verify the theoretical expressions and partly clarify the effect of various factors (number

[1a] McGowan, W.M.: Explanatory Tests of a Nailed Plate Connector for Glued Laminated Construction. Forest Products Laboratory, Vancouver. Information Report VP-X-11.

[1b] McGowan, W.M.: A Nailed Plate Connector for Glued Laminated Timbers. Journal of Materials, Vol. 1, No. 3.

of pins, number of pins in direction of force, distances from ends, pre-drilling, loading time, climatic conditions).

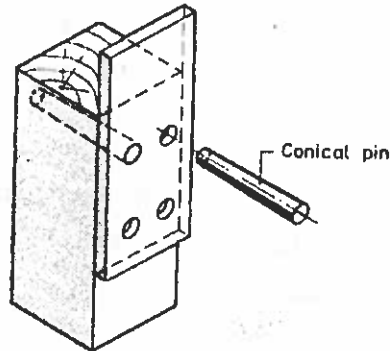


Fig. 1.

THEORY

Yield load.

The general basis is given in [2]. The theoretical appearance of the joint, corresponding to the type of yielding aimed at (denoted III in [2] fig. 06) is shown in fig. 2.

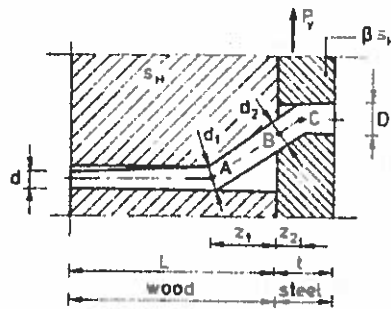


Fig. 2.

The yield point A in the wood lies at a distance z_1 from the surface of the wood. When z_1 is known, the diameter at A can be determined on the basis of the known D and the conicity of the pin (which is normally 1:50). The yield moment at A is

$$M_{yA} = \sigma_y d_1^3 / 6$$

[2] H.J. Larsen: Yield Load of Bolted and Nailed Joints, IUFRO, 1973.

where σ_y is the yield stress.

Over the length AB we assume a constant loading

$$s_H(d_1 + d_2)/2$$

where s_H is the embedding strength.

As z_2 proves to be very small, the diameter is assumed to be constant and equal to d_2 over the length BC, i.e. the yield moment at C is

$$M_{yC} = \sigma_y d_2^3 / 6$$

If we designate

$$\beta = \frac{\sigma_H d_2}{s_H(d_1 + d_2)/2} \quad (1)$$

where σ_H is the embedding strength in the steel gusset, the yield load will be determined from formula (16) in [2], with $2M_y$ substituted by $(M_{yA} + M_{yC})$ and $2d$ by $(d_1 + d_2)$, i.e.

$$P_y = \sqrt{\frac{\sigma_y s_H}{6}} (d_1^3 + d_2^3) (d_1 + d_2) \frac{\beta}{1 + \beta} \quad (2)$$

Assuming that the shear force is zero at the yield points A and C, we find

$$P_y = s_H z_1 (d_1 + d_2) / 2 \quad (3)$$

and

$$P_y = \sigma_H z_2 d_2 \quad (4)$$

P_y can be determined from (1) - (3) when the geometry of the pin and the material strengths are known.

It is a condition that l and t are so large that yield type II, with yield point in the wood or the steel, cf. fig. 7 in [2], cannot occur. The necessary criteria will not be derived here; however, approximating, we find

$$l_{\min} = 4 \cdot \sqrt{\frac{M_{yC}}{s_H d_2}} \quad (5)$$

and

$$t_{\min} = 2.4 \cdot \sqrt{\frac{M_{yC}}{\sigma_H d_2}} \quad (6)$$

Slip at working loads.

At normal working loads, the conditions can be assumed to be linear-elastic, and the slip can, as an approximation, be found by considering the pin as an elastic beam that is free to move but restrained at the surface of the wood and resting on an elastic support.

Approximating the bending stiffness EI of the pin by $E \frac{\pi d_2^4}{64}$ and writing the reaction to the pin as $p = Ky$, where $y = y(x)$ is the impression, see fig. 3, we find the slip g at the surface [3] to be

$$g = \frac{P}{k_y} \quad (7)$$

where

$$k_y = \sqrt{2} \cdot K^{\frac{3}{4}} \cdot (EI)^{\frac{1}{4}} = 0,67 \cdot K^{\frac{3}{4}} \cdot E^{\frac{1}{4}} \cdot d_2 \quad (8)$$

or

$$\frac{K}{E_t d_2} = 1,72 \cdot \sqrt[3]{\frac{k_y^4}{E \cdot E_t^3 d_2^7}}$$

where P is the force per pin and E is the modulus of elasticity of the steel, and E_t of the wood.

TESTS WITH PINS

Conical steel pins complying with German standard DIN 1 were used for the tests. The pins are supplied in many different sizes, designated by $d \times L$, where d is the minimum diameter and L the length, see fig. 4. Regardless of size, all the pins have the conicity 1:50.

[3] Troels Brøndum-Nielsen: Spændbetontanke, 1964.

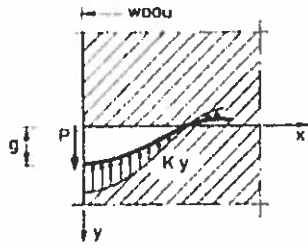


Fig. 3.

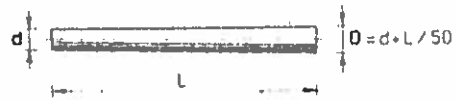


Fig. 4.

Pins with the dimensions 2.5 x 50 mm and 6.5 x 100 mm were selected for the tests.

The pins have a guaranteed minimum tensile yield strength (stress) of 500-600 N/mm². The actual yield moments, M_y , were determined by means of an arrangement as shown in fig. 5.

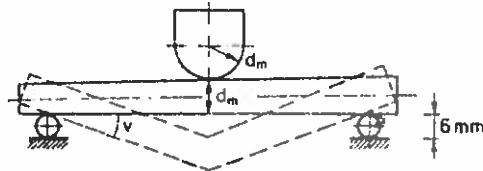


Fig. 5.

There are quite heavy deflexions, and in the calculation of the moment at the middle, the alteration in the geometry due to the deflexions is taken into account.

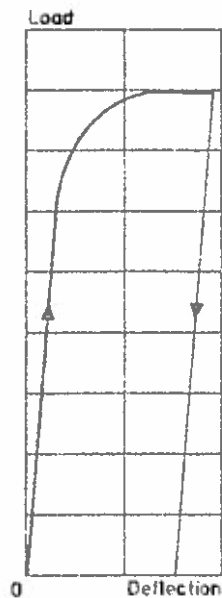


Fig. 6.

A typical stress-strain curve is shown in fig. 6. It will be seen that the force remains constant over a length, which - because of the alteration in the geometry - means that the stress increases very slightly (strain-hardening). It was therefore necessary by definition to fix the angle v , see fig. 5, at which the yield stress is calculated. On the basis of tests on the joints, a value of $v = 20^\circ$ was adopted for the 2.5 mm pins, and a value of $v = 15^\circ$ for the 6.5 mm pins.

The yield stress σ_y is calculated on the basis of the yield moment M_y as

$$\sigma_y = M_y/W_p = M_y/(d_m^3/6) \quad (9)$$

where W_p is the plastic moment of resistance. The calculated yield stresses etc. are given in table 1.

Table 1.

Dimension mm x mm	Batch No.	Yield stress in bending N/mm ²		No. of samples
		Mean	Stand. div.	
2.5 x 50	1	1018	20	20
	2	922	26	15
	3	996	20	15
6.5 x 100	1	688	16	15

TESTS ON JOINTS

Test programme

The test programme is shown in fig. 7.

The tests aimed at clarifying the effect of the following factors:

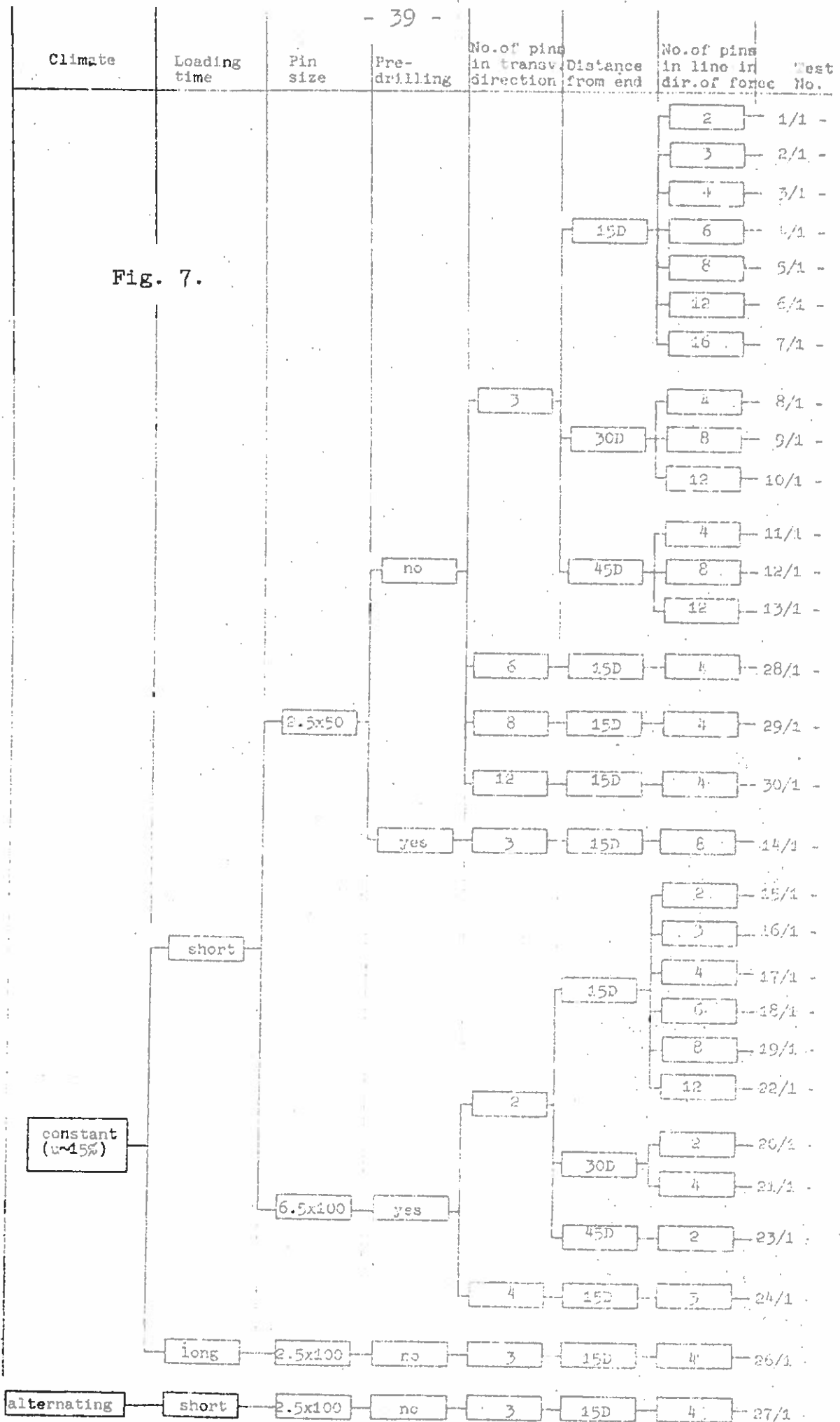


Fig. 7.

- Climatic conditions:** In the majority of the tests a constant moisture content (about 15%) from nailing to testing was aimed at. In a single test series the effect of alternate wetting and drying was investigated.
- Loading time:** Most of the tests were carried out as short-term tests, in which the load was increased from zero to failure in the course of 6-8 minutes. In a single series, the joints were subjected to constant loading, and the development of slip in relation to the time was measured.
- Pin size:** Two pin sizes were used, corresponding to the extreme limits of the sizes likely to be used in practice.
- Pre-drilling:** In the case of small pins, it was investigated whether the bearing capacity and stiffness were increased by pre-drilling instead of nailing the pins straight in. For the big pins it was absolutely essential to pre-drill.
- No. of pins:** It was investigated whether the bearing capacity depended on how many pins were placed beside each other (at right-angles to direction of force) and on how many pins were placed in line (in direction of the force).
- Distance from ends:** Most of the tests were carried out with the standard value for ordinary nailed joints, i.e. $15D$, where D is the largest diameter. It was investigated whether an increase in the distance to $30D$ or $45D$ resulted in an increase in the bearing capacity.

Each test series comprised 5 joints, except series No. 26, in which there were 9 joints, and series No. 27, in which there were only 4. A total of 148 joints were tested.

The minimum spacings specified in the Danish Code of Practice for Timber Structures for steel to timber were used throughout, i.e. $7D$ between the pins in the direction of the force and $3.5D$ between the rows of pins at right-angles to the force, and $5D$ from centre of pin to edge of wood.

Short-term tests

5 mm steel gussets were used for the 2.5 mm pins, and 13 mm gussets for the 6.5 mm pins. Holes with a diameter 0.2 mm smaller than the largest diameter of the pins were pre-drilled in the plates. At a difference in diameter of 0.1 mm, the introductory tests showed that there was a risk of the pins passing right through the plate, while at a difference of 0.3 mm, it was very difficult to hammer the pins sufficiently far in to obtain a smooth surface.

The wood used, which was Scandinavian spruce or pine, was conditioned at room temperature and a relative humidity of 75%. Test series No. 27 was an exception to this. Here, the specimens were submerged in water to fibre-saturation and then dried to a moisture content of 7-8%. This procedure was repeated seven times. However, after the last wetting, the moisture content was only reduced to about 15%, after which normal testing was carried out.

The small pins were either hammered straight into the wood or were hammered in after pre-drilling with a 2.5 mm drill, i.e. corresponding to the minimum diameter.

Pre-drilling was absolutely essential for the big pins. When holes were pre-drilled with a 6.5 mm drill, damage often resulted (splitting of the wood), and a 7.0 mm drill was therefore used over the whole length. The holes were thus slightly larger than the pins over a length of about 25 mm. However, this should be of no significance, partly because the hole is partly filled due to compression of the wood during hammering-in of the pin, and partly because the outer 25 mm are of very

little importance to the functioning of the pin.

The load (tension) was transmitted to the wood through a bolted steel plate. This plate and the steel gusset forming part of the joint were fixed directly in the grips of the testing machine and were shaped in such a way that the force lay in the joint between wood and steel, cf. fig. 8.

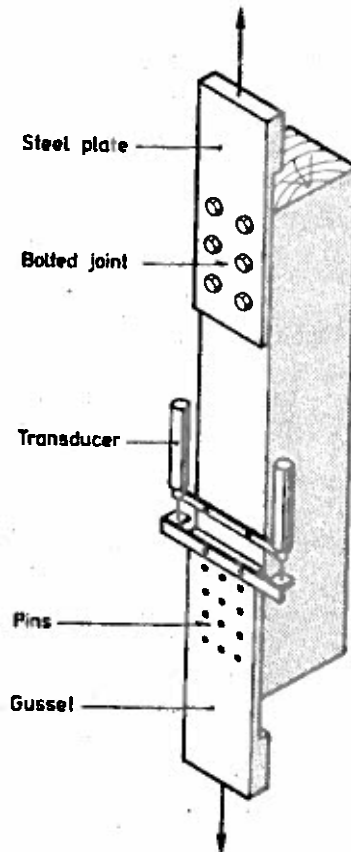


Fig. 8.

The tests were carried out on the Department's Mohr-Federhaff hydraulic 60 Mp universal testing machine. The force was registered electronically.

A constant pump output was used, i.e. the load was increased as something between constant loading rate and constant rate of deformation. The equipment for the machine at the time of testing did not permit the load to be increased corresponding to constant rate of deformation, which is normally considered

preferable. From the rupture conditions it is estimated that this has no effect on the maximum loads achieved, but that it did perhaps affect the appearance of the stress-strain curves around maximum loading.

The slip was measured by means of two transducers (Hewlett-Packard HP-7DCDT-1000), placed on a metal plate screwed to the wood and with the feeler on a bridge fixed magnetically to the gusset. The measuring length was about 20 mm. The elongation of the wood over this length is infinitesimal in relation to the slip.

The signals from the force and deformation measurements were transmitted to a printer, which traced the stress-strain curves direct.

After each test, the moisture content was determined by means of an electrical moisture-meter (Delmhorst), calibrated by determining the moisture content in about 60 cases by weighing and drying. The moisture content lay between 14% and 20%, average 16%.

After each test the specific weight was also determined by means of an approximately 5 cm thick slice cut from the entire cross-section of the wood. The specific weight was determined corresponding to weight and volume at a moisture-content of 15% (ρ_{15}). The specific weight lay between 330 and 640 kg/m³, average 490.

Long-term tests

A total of 9 long-term tests were carried out, designated 26/1 - 26/9. The number of pins, intervals, etc. are shown in fig. 7. The test specimens were as in the short-term tests, except that the transducers (fig. 8) were substituted by dial gauges (1/100 mm).

The load was applied through a lever arrangement and corre-

sponded to about 30% (26/1 - 26/3), 45% (26/4 - 26/6) and 60% (26/7 - 26/9) of the expected short-term strength.

The specific weight of the wood was determined, and the slip was registered over a period of about 12 months.

The tests were carried out in a room with a rather constant climate, corresponding to 20°C and a relative humidity of about 50%, which gives a moisture content of the wood of about 10%.

TEST RESULTS

Typical stress-strain diagrams are shown in fig. 9-10 and the typical appearance of the joints after failure is shown in fig. 11, the wood being split along a row of pins after the test.

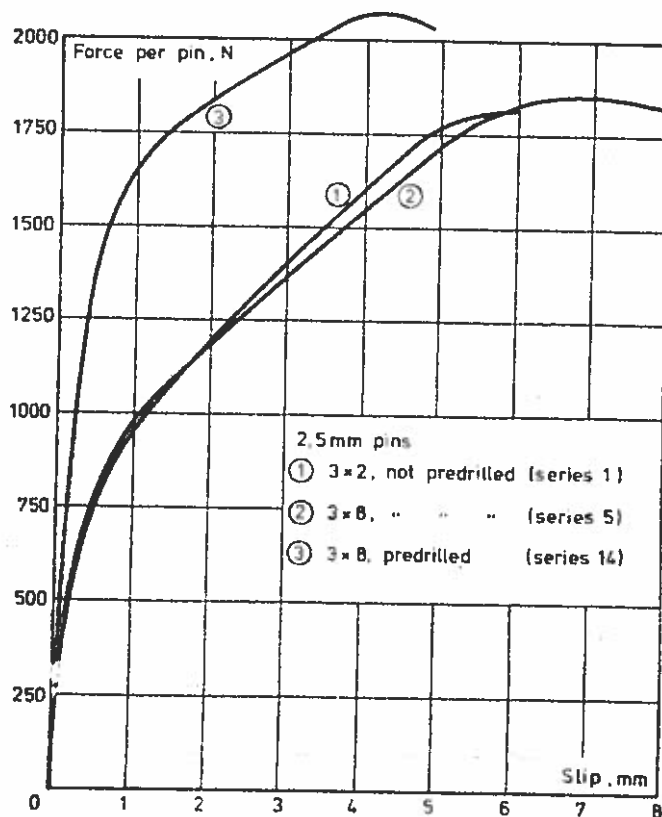


Fig. 9.

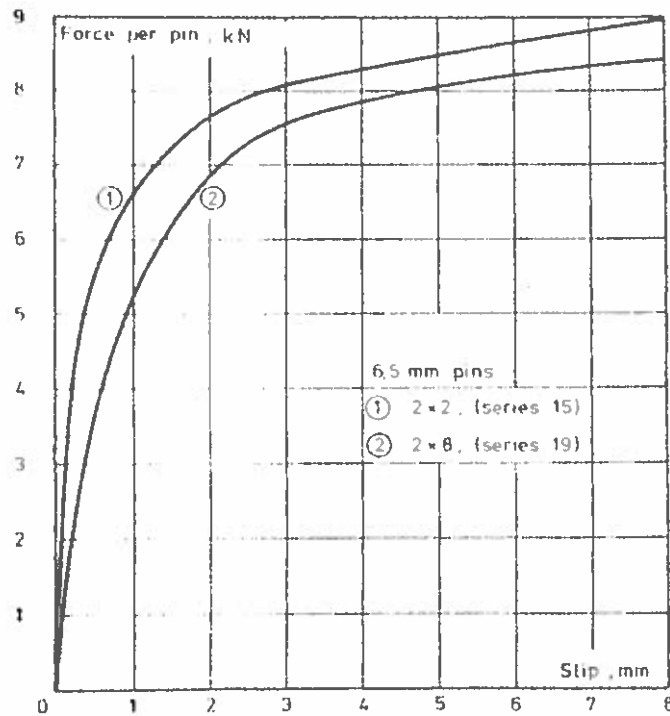


Fig. 10.

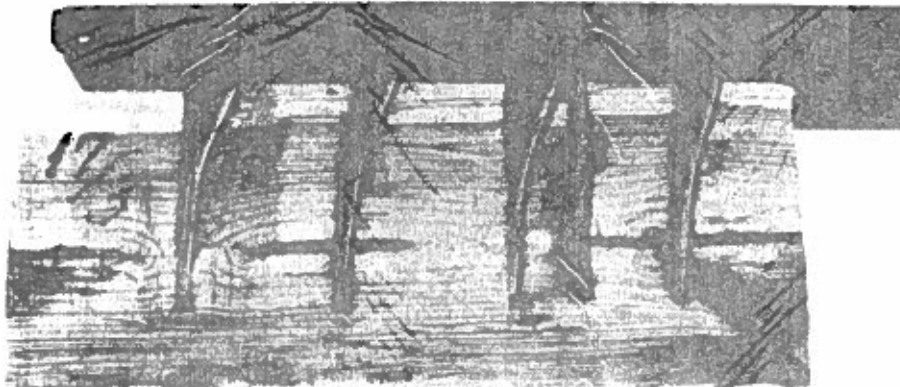


Fig. 11.

Strength values

The complete test values etc., are given in [4].

The directly measured yield loads, P^m , per pin are compared in the following with the theoretical value P^t for the joint in question.

P^t is calculated by means of formulae (1)-(3).

[4] Structural Research Laboratory, Technical University of Denmark. Intern Rapport, No. 1-24.

As β (formulae(1)) is of the order of magnitude 20, and the bearing capacity (formulae(2)) depends on β $(1+\beta)$, it will be seen that it is not necessary to know σ_H exactly. Therefore, corresponding to the assumption in steel structures, σ_H is tentatively put at double the yield stress for the gussets, which are of steel st. 37, i.e. at $2 \cdot 240 = 480 \text{ N/mm}^2$.

In accordance with [6] and formulae (6.42) and (1.10) in [5], the embedding strength s_{Hu} can be determined from the following empirical expressions valid for $\frac{d_1+d_2}{2} \leq 6 \text{ mm}$:

$$\begin{aligned} s_{Hu} &= 0.09 \left(14 - \frac{d_1+d_2}{2} \right) s_{Pu} \\ &= 0.09 \left(14 - \frac{d_1+d_2}{2} \right) \frac{s_{p15}}{0.10 + 0.06 \cdot u} \\ &= 0.09 \left(14 - \frac{d_1+d_2}{2} \right) \frac{0.087 \rho_{15}}{0.10 + 0.06 \cdot u} \end{aligned} \quad (10)$$

For $d_2 > 6 \text{ mm}$, it is assumed, in accordance with the same references, that

$$s_{Hu} = 0.7 s_{Pu} = 0.7 \frac{0.087 \rho_{15}}{0.10 + 0.06 \cdot u} \quad (11)$$

where s_{Pu} is the prism strength at a moisture content u (%), and ρ_{15} (kg/m^3) is the density calculated on the basis of the weight and volume at a moisture content of 15%.

Unless otherwise directly stated, the values given for P^m/P^t are the average values for each series of 5 tests.

In cases in which it is stated that there are significant differences, at least a 95% criterion is used.

For the small pins, the characteristic yield load was of the order of magnitude of 15 kN per pin, while for the big pins, it was about 75 kN per pin.

Evaluation of strength results

Effect of pre-drilling. For series 5 it was found that P^m/P^t

[5] Larsen, H.J.: Materialer og Forbindelsesmidler til Trækonstruktioner, 1971.

[6] Nielsen, T. Feldborg og Marius Johansen: Forsøg med træforbindelser med bolte og mellemlæg. Statens Byggeforskningsinstitut, Rapport nr. 67, Copenhagen 1970.

= 1.03 (standard dev. = 0.03), and for series 14, P^m/P^t = 1.26 (s.d. = 0.11). The two series were identical apart from the fact that pre-drilling was used in series 14. In view of the deviations found, the difference is significant.

Effect of number of pins at right-angles to direction of force: Fig. 12 shows the values of P^m/P^t found for series 8, 28, 29 and 30. These were identical except that the number of pins (2.5 x 50 mm) at right-angles to the direction of the force varied from 3 to 12.

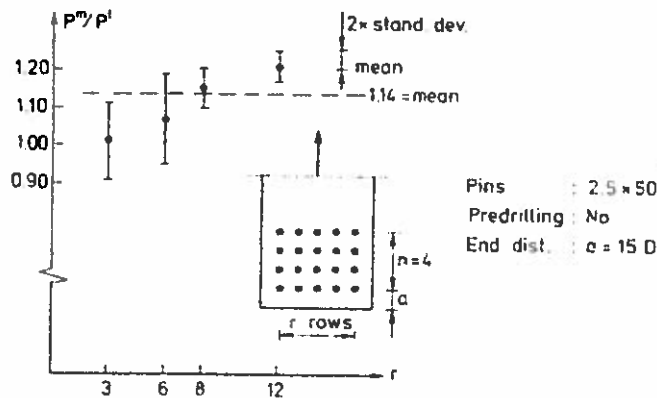


Fig. 12.

It will be seen that the bearing capacity increases with the number of rows, which is inexplicable and must be fortuitous even though, evaluated statistically, the phenomenon is significant.

For the two comparable series for the 6.5 x 100 mm pins, P^m/P^t was found to be 1.22 for series 16 (2 rows), and 1.02 for series 24 (4 rows) which is a significant fall. However, the wood in series 24 had quite considerable cracks, which partially explains the lower value.

Effect of distance from ends: Fig. 13 shows the effect of the distance from the ends. It will be seen that the chosen minimum distance of 15D is sufficient for the achievement of the full

bearing capacity.

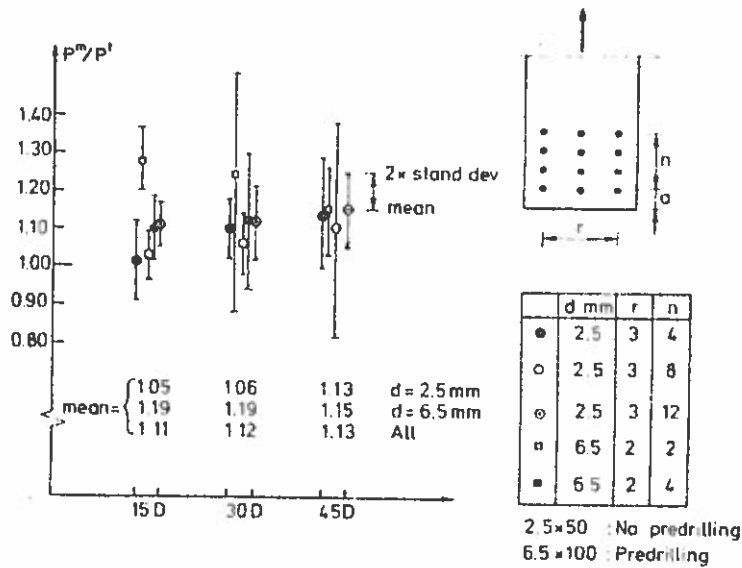


Fig. 13.

Effect of number of pins in direction of force: In fig. 14, P^m/P^t is plotted in relation to the number of pins in the direction of the force (n). As no relationship was found with the number of pins perpendicular to the direction of the force or with the distance from the ends, the results from all test series are included, apart from series 14 (where pre-drilling was used for the small pins) and 26-27.

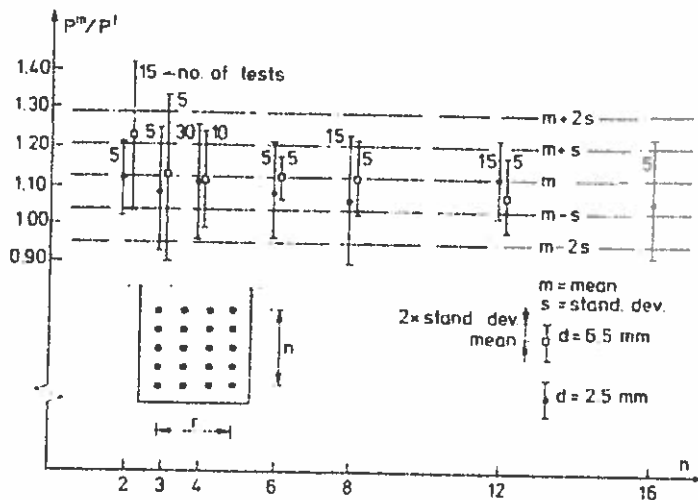


Fig. 14.

The mean for P^m/P^t (125 specimens) was 1.12, with a standard deviation of 0.086, i.e. a coefficient of variation of 7.6%. No single series deviated significantly from this mean. The mean for small pins was 1.10 (st. dev. 0.073) and for the big pins, 1.15 (0.10).

Effect of alternating moisture content: In the single test series (No. 27) in which the moisture content was varied, a significantly higher bearing capacity was found. (But also a considerably bigger deformation).

Stiffness values

On the basis of the individual stress-strain diagrams the slip was determined corresponding to normal working load, which was estimated to be 35% of the yield load.

The movements showed a rather big variation, which was only to be expected since they are closely related to possible friction.

For the small pins, the movements averaged 0.24 mm for joints with 6-12 pins, while for more pins, they averaged 0.30 mm. The exceptions to this are the pins with pre-drilling, where the movements were only 0.14 mm, and the joint exposed to variations in moisture, where the movements were 0.56 mm.

For the big pins, the movements for joints with 4-6 pins were 0.13 mm; for 8-12 pins, 0.20 mm; and for more than this, 0.27 mm.

For joints with a large number of pins, k_y (formula (7)) was of the order of magnitude of 2100 N/mm for small pins, and 9000 N/mm for big pins.

Fig. 15 shows $\frac{K}{E_t d^2}$, in accordance with formula (8), where E_t is the modulus of elasticity of the wood, estimated according to [7] on the basis of the density,

[7] Schlyter, R. and G. Winberg: Svensk Furuvirkes hållfasthetsegenskaber. Ingeniørvetenskabsakademiens Handlinger Nr. 92, Stockholm 1929.

$$E_t \sim 41.5 (\rho_{15} - 230) \text{ N/mm}^2 \quad (12)$$

For the material used, E_t lies between 8000 and 17000 N/mm^2 .

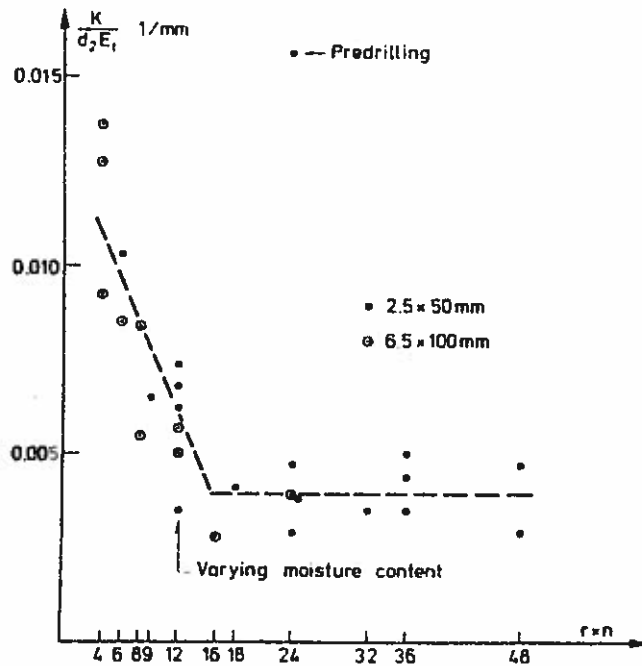


Fig. 15.

It will be seen that $\frac{K}{E_t d_t^2}$ is of the order of magnitude of 0.0039 1/mm for the number of pins exceeding 12; while the stiffness for smaller numbers is considerably greater.

Long-term tests

Fig. 16 shows the development of the slip with time. Relative values are used, the slip at the time $t = 1$ minute, when the first reading was taken, being put at 1.0. The actual movements at this point of time were about 0.2 mm for a loading level corresponding to about 30% of the expected yield load, 0.80 mm for a loading level of about 45%, and 1.80 mm for a loading level of about 60%.

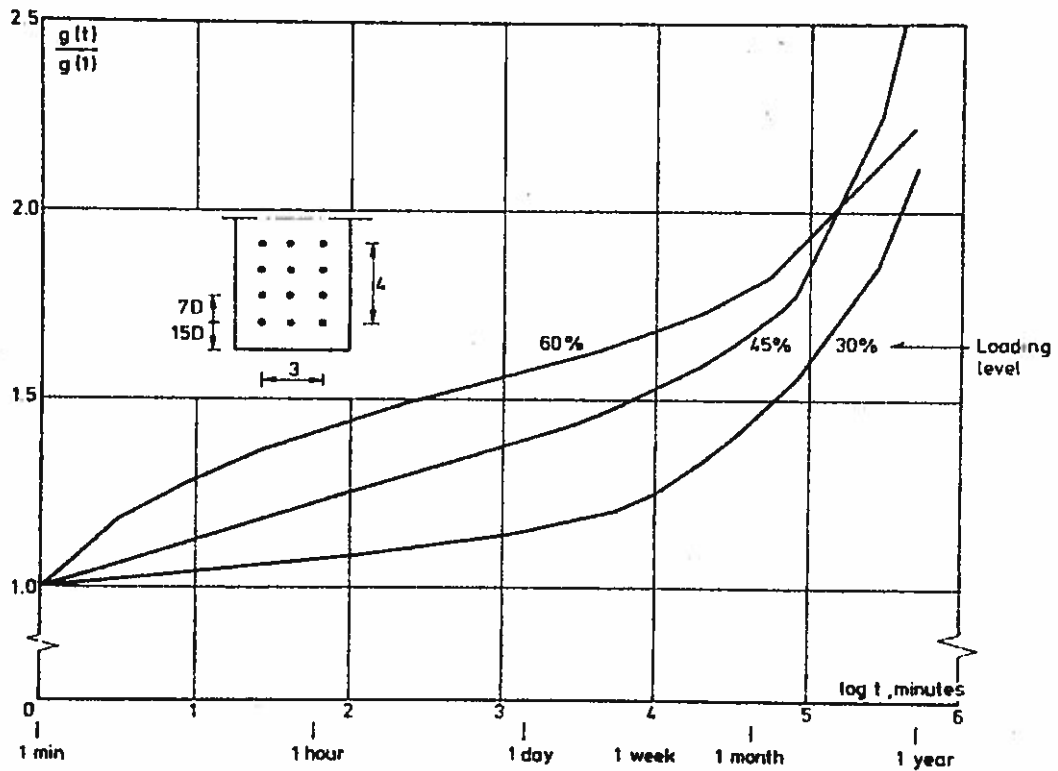


Fig. 16.

For the loading level corresponding to 30% of the yield load, the slip amounted to less than 0.5 mm after about a year. This should be seen in the light of the fact that the yield slip are of the order of magnitude of at least 5-6 mm. Even if the slip was to continue to accelerate (in the chosen single-logarithmic depiction) there would be no risk of failure during the lifetime of a structure.

In the subsequent short-term tests it was found that the ratio between the measured bearing capacity and the theoretical capacity, P^m/P^t , was 1.07, i.e. the foregoing long-term testing did not reduce the strength significantly.

The movements under normal working loads were perhaps slightly higher than in the corresponding short-term specimens, but the small number of specimens does not allow us to exclude the possibility of this being fortuitous.

CONCLUSIONS

The type of joints investigated appear to be suitable for large connexions, joints in glulam beams etc.

The ratio between the yield loads found by means of the tests and the theoretical values is 1.12, with a coefficient of variation of about 7.5%. That the test values are somewhat too high is due to the fact that the theoretical expressions neglect friction forces and that part of the load in the vicinity of failure can be taken as tension in the pins lying in an inclined position.

The bearing capacity per pin was found to be the same, regardless of the number of pins per joint, even when there was a large number of pins (up to 16) in a row. This really seems reasonable if we compare the movements occurring near rupture with the deformations that can occur in the gusset between the pins. That it has been found, for example for Glulam Rivets [1b], that the bearing capacity decreases with the number of rivets is presumably due to the fact that considerably smaller spacings have been used with these, so that rupture in the case of the big quantities of rivets occurred as shear failure in the wood in a plane through the yield points A (see fig. 2). In the present tests, such large spacings were used that the strength of the wood did not constitute a limiting factor.

The movements under service conditions are small for short-term loads (a few tenths of a mm, maximum for the small pins), but the joint still shows good plastic properties near rupture (movements of 5-6 mm). Under long-term loading, the movements increase (slightly more than doubled in the course of one year), although without such serious creep as to endanger the long-term strength.

The movements are independent of the number of pins when this exceeds about 12, but are reduced when fewer pins are used. This is only to be expected since with the large number of pins,

the load will be distributed unevenly over the pins under normal working conditions.

Pre-drilling results in a considerable increase in both the strength and the stiffness.

The end distances adopted (15 x the diameter) and the pin spacing (about 7 x the diameter in the direction of the force and about 3.5 x the diameter perpendicular to this) are sufficient for the achievement of the full bearing capacity.

Prior long-term loading does not entail any deterioration of the short-term properties.

STRUCTURAL FAILURES IN DENMARK 1971-73

H.J. Larsen

Structural Research Laboratory
Technical University of Denmark.

* * *

The most remarkable type of structural failure has been the destruction of a number of glulam pitched cambered beams in four or five buildings, see fig. 1.



As several similar cases have already been reported, cf. inter alia [1], it will suffice just to repeat a few characteristic features:

1. The construction material is Scandinavian spruce, the characteristic short-term tensile strength of which, perpendicular to grain, is 0.9 N/mm^2 , and for which the current Code of Practice For the Structural Use of Timber [2] reckons with a long-term factor of 0.6 and a safety factor of 1.8, i.e. the permissible stress is 0.3 N/mm^2 .
2. The stresses perpendicular to grain were originally calculated from the expressions applying for a curved beam of constant height (broken line in fig. 1), and are found to be 0.10 N/mm^2 both for dead load and for snow load, giving a total of approx. 0.20 N/mm^2 .
3. If (as specified by Foschi and Fox [3]), the changes in the stress field caused by the triangle at the top are taken into account, these stresses will be increased by a factor of 2.7, i.e. to 0.54 N/mm^2 . Thus, formally, the beam is unacceptable, and had the rupture occurred after the structure had been subjected to full snow load for a long time, the failures would have been understandable.
4. However, the rupture occurred about 18 months after erection, without the structure having been exposed to snow load of any significance, and the stresses never greatly exceeded the permissible stress and were, in fact, below this for most of the time.

5. The reason for the failures is presumably that, as established in [1], the long-term reduction is considerably greater than assumed. A contributory factor has presumably also been moisture stresses, which may be quite considerable in the big cross-section in question (about 200 x 2000 mm). The damage occurred mainly in the spring, when the timber is moistened from the outside, and the moisture content in the outer 10-20 mm was found to be 3-5% higher than inside the beam.
6. Although quite considerable cracking occurred (up to 100 mm wide) no cases of actual collapse have been reported. Either a favourable rearrangement of the stresses has taken place after rupture or a part of the load has been taken by the diaphragm effect in the roof surfaces.
7. The buildings in question have been reinforced by means of prestressed ties - an ironic solution in view of the fact that the pitched cambered beam solution was adopted precisely to avoid the use of ties.

*

The number of structures damaged - possibly collapsed - is otherwise presumably considerable, but in most cases the reason was to be found in obvious errors - of calculation, design or execution - and the cases were settled discreetly between the parties, possibly through the mediation of insurance companies. This is really unfortunate because even though the cause of the damage is clear, useful information could in many cases be obtained on the carrying capacity of the structures and possibly also on the reasonableness of the load assumptions.

* *

- [1] Madsen, Borg: Duration of Load Tests for Wood in Tension Perpendicular to Grain. The University of British Columbia, Structural Research Series. Report No. 7, 1972.
- [2] Danish Standard DS 413, 2nd edition, 1968.
- [3] Foschi, R.O. and Fox, S.P.: Radial Stresses in Curved Timber Beams. Journal of the Structural Division, Vol. 96, ST 10, Oct. 1970.

NOTE ON DETERMINATION OF CHARACTERISTIC VALUES

H.J. Larsen and H. Riberholt
Structural Research Laboratory
Technical University of Denmark

* * *

POLEMIC SURVEY AND INTRODUCTION

In recent years it has been agreed that permissible stresses etc. shall be fixed on the basis of a characteristic value, i.e. a low probability limit for the strength values. Using statistical terminology, the characteristic values must thus be determined as a fixed fractile in the distribution function for the quantity investigated.

There is not yet complete agreement on the fractile to be used, but as far as wood is concerned, it looks as though the 5% fractile is being accepted for values for strength calculations.

The application of statistically determined characteristic values facilitates the specification in building codes and standards of the requirements to be complied with, but problems arise when the general requirements are to be utilized in practice.

Only in cases of a very large number of samples is the determination of the characteristic value free from problems because then it can be assumed that the real population and that constituted by the samples are identical.

If the distribution function is known, then it will be possible to calculate the fractiles, even in the case of a limited number of samples. Further uncertainty admittedly arises because the sample population does not necessarily have the same properties as the real population, but there are recognized statistical methods for taking this into account, for example, by determining the 5% fractile with a desired probability or, more correctly, corresponding to a desired confidence level.

Agreement has not yet been reached on what can be considered a reasonable figure for this confidence level. In Denmark, a 75%-level is used, while in Canada, it appears from [1] that a 95%-level is being considered.

Unfortunately, we only have the necessary knowledge of the distribution functions in a few cases. This applies, for instance, to manufactured products such as chipboard and fibre-board, where certain strength values are determined as a routine procedure, and perhaps also to certain short-term

strength values for the commonest types of wood. However, these are exceptions; the distribution function is normally unknown and, for reasons of economy, there is usually only a limited number of samples. In this event it is often impossible to determine the characteristic value with a reasonable degree of certainty.

In many instances, the problem is neglected, and the Normal distribution is assumed; this frequently gives reasonable results - subjectively evaluated, either because the distribution does happen to be approximately normal or because the standard deviation is so small that the distribution assumed is completely immaterial.

In cases in which these conditions are not fulfilled, the results may be totally unreasonable, both from an objective evaluation (e.g. when negative strengths are found or when the addition of further test values, that happen to be quite high, result in a reduction of the characteristic value) and subjectively, because one "knows" intuitively that the results are unreasonable. A number of depressing examples of the consequences of an incorrect application of the Normal distribution are given in [1].

When our elementary knowledge of statistics proves insufficient, we have no alternative but to pocket our pride and turn to the specialists. But that rarely helps. The statisticians simply assert that the problem is insoluble and refuse to waste more time on it.

Now engineers hate to admit that there are insoluble problems and they attribute the attitude of the statisticians to ill-will or ignorance, whereupon they take it upon themselves to solve the problems. When the specialists have given up, there is room for intuition and talented amateurs.

To the intuitive belongs the notion that there really is a "distribution" common to all wood-based materials and structures. All you have to do is find it.

However, when we begin to collect the necessary material to determine the "distribution" we rapidly lose our illusions. Some distributions are symmetrical, others are unbalanced, with an excess of low results, and still others are unbalanced with an excess of high results.

On reflection, it does seem probable that there is difference in the distribution in respect of, for instance,

- natural products, where no grading has been carried out,
- natural products graded to remove particularly low values,
- natural products graded into classes,

- manufactured materials,
- glued, composite constructions,
- composite constructions assembled with mechanical fasteners (for example, trusses).

The probability of it being reasonable to use the normal distribution will be highest for the manufactured materials and for composite constructions whose properties are not systematically dependent on the properties of a single element.

Another intuitive feeling is that the distribution functions must have certain common properties even though they differ, and that it must be possible to use these to determine the fractile sought. It does not appear directly probable - after all, the difficulty lies in the fact that the determination becomes very uncertain when the distribution function is not known - but still!

[1] is a comprehensive work based on the assumption of these common properties and, despite an instinctive scepticism, the investigation does indicate that such properties do exist, e.g. that the determination of a given fractile with a required confidence level can in all events be replaced by the determination of another, smaller fractile with a confidence level of 50% (mean value).

Unfortunately, however, a number of objections can be made to the investigation in question. First, the most important of the sets of data used does not satisfy the requirement that all the test values must belong to the same population because the test conditions - and especially the loading rate - vary. Secondly, the data material is very modest. Although data-sets of 200-300 seem impressive at first glance, they are, in fact, totally inadequate as a basis for fixing confidence levels - which is what is done here. The fact that colossal quantities of figures are generated by means of EDP can never compensate for the inadequacy of the basic material.

Although harbouring great scepticism with regard to the possibility of determining the characteristic value with the required degree of accuracy on the basis of a limited quantity of test data, the problem is so important that we must leave no stone unturned, and the following is therefore proposed:

ACTION PROGRAMME

1. Data are collected from test series in which the same tests are repeated many times, great importance being attached to ensuring that all data from a series in a data-set are generated from one and the same statistical process.

A number of the test series in [1] satisfy this requirement and can be used.

2. Each data-set is tested with a view to ascertaining the distribution that best describes the set.

First it is investigated whether certain of the standard distributions (Normal, Log-normal, Kapteyn) can be used. If this is not the case, a simple transformation is sought that can lead the test results over to one of the standard distributions.

What we achieve by tying ourselves to one of the standard distributions is that once we have found an acceptable transformation, we can carry out the rest of the statistical treatment and description with clear mathematical stringency, no further approximations have to be introduced.

The method used in [1] cannot be recommended, firstly because information on the appearance of the distribution gets lost when the method with weighting of data is used, and secondly, because it is impossible to assess the degree of inaccuracy on the results achieved when a number of approximations are made during the numerical treatment.

3. We investigate which transformation (distribution) best describes either all or groups of the data-sets. Here, we may, for example, find that one transformation is best in the case of bending, while another is best in the case of shear.
4. When the most probable transformations (distributions) have been found, whether these be transformations for general application or for specific problems such, as for instance, bending or shear, they are generally used for the problem in question, even for a limited number of samples.

EXAMPLE

In order to illustrate the action programme, a number of data-sets from different tests have been investigated.

In order to ascertain which distribution was best, the data-sets collected were tested by means of the χ^2 -test, in which data are "ranked" and divided into k groups. The number in each group a_i are counted, and by means of the assumed distribution, the number $n \cdot \theta_i$ which ought to be in each group according to this is determined. χ^2 is then defined by

$$\chi^2 = \sum_{i=1}^k \frac{(a_i - n\theta_i)^2}{n\theta_i}$$

By means of standard tables, for example from [2] or [3], the fractile to which the relevant value corresponds is determined. The results are shown in table 1, where the fractiles in χ^2 give the probability of finding values of χ^2 lower than that found, i.e., a big fractile means that the distribution function provides a poor description of the data-set and thus,

with a certain probability, a poor description of the problem under consideration.

TABLE 1

Data-set No.	Number of data n	Normal distribution			Log-normal distribution		
		Degrees of freedom f	χ^2	Fractile in χ^2	Degrees of freedom f	χ^2	Fractile in χ^2
1	241	10	31,3	99,95	12	28,8	99,5
2	195	6	2,41	12	7	5,17	38
3	189	11	12,7	69	12	48,1	99,95
4	285	14	59,4	99,95	13	57,1	99,95
5	206	14	50,0	99,95	14	29,7	99,1
6	68	4	27,5	99,95	4	8,91	94
7	68	4	11,59	98,4	4	5,56	76
8	63	4	12,94	98	4	4,31	63
9	60	4	17,5	99,6	5	7,7	80,2

1. Compression of small clear specimens, Lars Bach, Dth Denmark.
2. Bending of 63 x 125 mm poorest grade in Denmark, H.J. Larsen & H. Riberholt, Denmark.
3. Clear Dry bending, Borg Madsen, Canada.
4. # 2 grade Dry bending, Borg Madsen, Canada.
5. # 2 grade Wet bending, Borg Madsen, Canada.
6. Shear of beam notched at the support, 1/4 height.
7. Shear of beam notched at the support, 1/2 height.
8. Shear of beam notched at the support, 3/4 height.
9. # 2 grade Dry bending, 1 min. Borg Madsen, Canada.

In order to illustrate visually what actually lies behind the χ^2 -fractiles, fig. 1 shows the distribution of the failure load for # 2 grade, dry bending, 1 min. (No. 9 in Table 1). From this it will be seen that the Log-normal distribution provides a better description than the Normal distribution, as indeed indicated by the χ^2 -fractiles in Table 1. The advantage of the χ^2 -test is that we get a quantitative evaluation of the distribution that best describes the data-set.

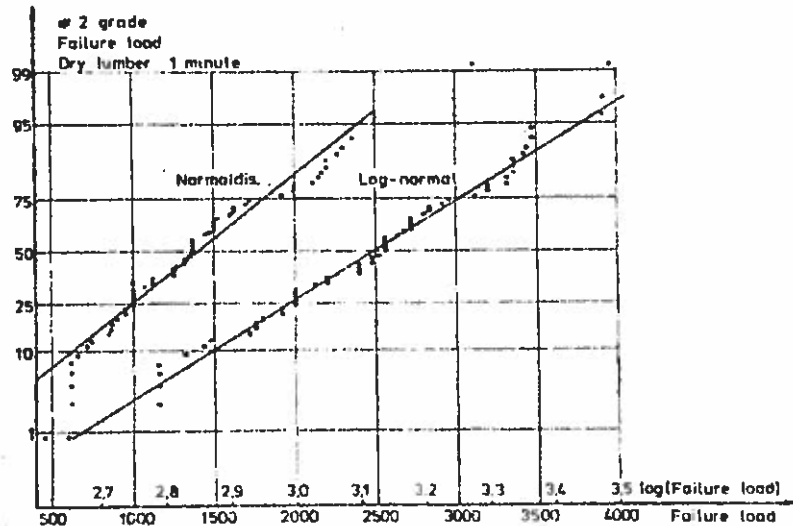


Fig. 1

The following conclusions can be drawn from Table 1:

- For data-sets No. 1, 6, 7 and 8, in which there has been no grading whatsoever of the material, the Log-normal distribution gives a better description than the Normal distribution.
- For data-set No. 2, which is graded visually, rejecting both the poorest and the best, both distribution give a good description.
- For data-sets No. 3, 4 and 5, it cannot be determined which of the distributions gives the best description, none of them being particularly good. This must be attributed to the fact that each data-set consists of data generated from different statistical processes, some of the values originating from long-term tests and others from short-term tests. This can be confirmed by investigating No. 9, which is a sub-group of No. 4, but comprises only short-term tests; here we find that the description is generally better and that the Log-normal distribution is the best.

The above conclusions are only drawn to illustrate principles. They are based on very few data-sets and the applicability of only two types of distribution is investigated. To fulfil the aim formulated under point 4 above, it would be necessary to investigate a large number of data-sets and several types of distribution.

* * *

- [1] An engineering approach to estimating the 5th percentile levels for structural properties of wood. Borg Madsen. University of British Columbia.
- [2] Introduction to Statistical Inference. E.S. Keeping. D. Van Nostrand, Princeton, New Jersey.
- [3] Statistical Theory with Engineering Applications. A. Hald, John Wiley & Sons.

CODE FOR SPECIFICATION OF STRENGTH AND
STIFFNESS VALUES FOR WOOD BASED BOARDS

Nordic Building Regulations Committee
Structural Timber Group

Translation of NKB Trækonstruktionsudvalgets
XII Retningslinier for fastsættelse af styr-
ke- og stivhedstal for træbaserede plade-
materialer, 1. april 1973.

Synopsis.

The use of wood based boards (plywood, particle boards, and fibre boards) in structures is still increasing, for instance in stressed skin elements and box beams, and as gusset plates.

The Working Group for Timber under the Nordic Committee on Building Regulations (NKB) has prepared the following rules for the fixing of strength and stiffness values taking into account the dependence of time for these quantities.

The fixing is based on a statistic estimation.

The rules form the base of detailed regulations in each of the Nordic countries, the safety systems of the countries still being heterogeneous.

Apart from the basic principles is in an addendum given examples of characteristic values for each type of plate.

1. General.

This code has been prepared as a joint Nordic basis for the specification of characteristic values for wood-based boards, i.e. plywood and particle and fibre boards.

For use in calculations, a safety factor in accordance with current, national regulations shall be added to the values.

Note:

The code contain a few provisions applying only to boarding. Apart from this, the rules are generally applicable to wood and wood-based materials.

2. Loading groups.

The loading classification (loading groups A, B, C^{*}) specified in Nordic Building Regulations Committee (NKB), Publication No. 7, 1967, is used.

3. Climate classes.

On the basis of the moisture conditions, the structures are assumed to be grouped in the following climate classes:

Climate class 1a. The moisture content corresponds to the indoor conditions in a permanently heated building without artificial air-moistening, i.e. with an average annual relative humidity not exceeding 40%.

Climate class 1b. The moisture content corresponds to conditions in which the relative humidity of the surrounding air only exceptionally, and then only for short periods (a few days), exceeds 65%.

Note:

The moisture content of ordinary conifers lies under

*) A = Long-time loading, including snow.
B = Medium-time loading.
C = Short-time loading; the most important load in this group is wind.

about 13%.

In addition to the structures grouped under climate class 1a, the following can also be included in this class:

- roof structures in cold, but ventilated attics over permanently heated buildings,
- boards in outer walls in permanently heated buildings, where the boards are protected by a well-ventilated tight cladding.

Climate class 2. The moisture corresponds to conditions in which the relative humidity of the surrounding air only exceptionally, and then only for short periods (a few days), exceeds 85%.

Note:

The following structures can be included in this class:

- structures in not permanently heated, but ventilated, buildings in which no activities particularly likely to give rise to moisture take place, for example, holiday houses, unheated garages and warehouses, together with service space,
- outer roof boarding,
- scaffolding, concrete formwork and similar temporary structures.

Climate class 3. All other climatic conditions.

4. Material requirements.

It is assumed that the boards are sufficiently resistant to the climatic action to which they are exposed and that they are manufactured, checked and marked in accordance with regulations approved by the building authorities of one of the Nordic countries.

5. Specification of characteristic strength and stiffness values.

The following characteristic strengths are used corresponding to loading group A:

$$\sigma_{k,05} (10^5)$$

As characteristic stiffness for use in strength calculations:

$$E_{k,05} (10^5)$$

As characteristic stiffness for use in deformation calculations:

$$E_{k,30} (10^4)$$

Here,

$\sigma_{k,f} (t)$ is the characteristic strength corresponding to the $f\%$ fractile at a loading time of t hours,

$E_{k,f} (t)$ is the corresponding characteristic secant modulus.

The characteristic values are determined corresponding to a confidence level of 75%.

Note:

The 75% confidence level means that the probability of the characteristic values estimated on the basis of random sampling being too low is 75%.

For climate class 1a, the strength and stiffness values are determined on the basis of specimens conditioned at a relative humidity of 40% and a temperature of 20°C; for climate class 1b: at 65% and 20°C; and for climate class 2: at 85% and 20°C. For climate class 3, saturated specimens are used. Other conditioning can be used provided conversion factors are known or determined.

It is permissible to determine $\sigma_{k,f}(t)$ as

$$\sigma_{k,f}(t) = k_{\text{time}} \cdot \sigma_{k,f}$$

where

σ_k is the characteristic strength determined on the basis of standardized short-term tests (i.e. of a duration of between 10^{-1} and 10^{-2} hours) and

k_{time} is a factor taking the influence of the time into account.

k_{time} is fixed on the basis of tests of such duration as to permit a reasonably accurate evaluation of the influence of time.

Note:

It is often possible to assume:

$$\sigma_{k,f}(t_1) - \sigma_{k,f}(t_2) = C(\log t_2 - \log t_1)$$

Addendum 1.1*

Particle boards complying with DIN 68763*

a. Application.

Particle boards satisfying the requirement of DIN 68763 to class V 20 can be used in climate categories 1a and 1b, while boards satisfying the requirements to class V 100 or V 100 G can also be used in climate category 2, assuming that the boards are suitable protected against climatic action.

b. Strength and stiffness.

For loading group A, the strengths and stiffnesses specified in the following table 1.1 can be used.

Note:

The values given in the table are calculated on the basis of the values specified in the above-mentioned standard, assuming $k_{\text{time}} = 0.40$ in climate class 1 and $k_{\text{time}} = 0.25$ in climate class 2, in relation to the test duration of about 10^{-2} hours specified in the standard. A coefficient of variation of 0.10 has been assumed.

For the loading group B, the strength values can be multiplied by 1.40, and for loading group C, by 1.80.

For loading combinations consisting only of loads expected to act with their full value during the entire lifetime of the structure, both the strength and the stiffness values must be multiplied by 0.7.

In a continuous glued joint between a plate (board) flange and a maximum 30 mm wide web, the value for plate shear can be doubled. It is assumed that the distance from web to edge of plate is minimum 30 mm (measured perpendicular to the longitudinal direction of the joint), that the free distance

*) Corresponding addenda will be prepared for other particle board qualities.

between parallel joints is minimum 60 mm, and that the joint is not subjected to tension perpendicular to the plane of the joint.

Table 1.1 Particle boards complying with DIN 68763
Characteristic stresses and stiffness values in MN/m²

	Climate class 1 ^{*)}			Climate class 2		
	Thickness in mm			Thickness in mm		
	8	16	22	8	16	22
	10	19	25	10	19	25
	13			13		
<u>Strength calculations.</u>						
Bending	8.0	7.0	6.5	4.0	3.6	3.2
Compression \neq	4.8	4.3	3.8	2.2	2.0	1.8
Compression $_$	3.6	2.7	2.7	3.6	2.7	2.7
Tension \neq	3.6	3.0	2.3	1.6	1.6	1.6
Tension $_$	0.12	0.11	0.09	0.07	0.07	0.07
Shear through thickness	2.7	2.3	2.0	1.1	0.9	0.7
Plate shear	0.45	0.36	0.36	0.27	0.27	0.27
E-modulus, tension and compression	1200	900	800	400	350	350
E-modulus, bending	1400	1100	900	600	500	500
G-modulus	600	450	400	200	170	170
<u>Deformation calculations.</u>						
E-modulus, tension and compression	1500	1200	1000	600	500	500
E-modulus, bending	1900	1500	1200	900	800	800
G-modulus	750	600	500	300	250	250

^{*)} In climate category 1a, the strength values can be multiplied by 1.1 and the stiffness values by 1.3.

Addendum 2.1

Swedish Fibreboard (k-boards)

a. Application.

Wood-fibre boards that at least fulfil the requirements of Authorization No. T 75/71 from Statens Planverk (The Swedish Building Authorities) can be used in climate classes 1a, 1b and 2, assuming that the boards are suitably protected against climatic action.

b. Strength and stiffness.

For loading group A, the strengths and stiffnesses specified in the following table 2.1 can be used.

Note:

The values given in the table are calculated on the basis of the values specified in the above-mentioned authorization, assuming $k_{\text{time}} = 0.40$ in climate class 1 and $k_{\text{time}} = 0.25$ in climate class 2, in relation to a test duration of about 10^{-2} hours.

For the loading group B, the strength values can be multiplied by 1.40, and for loading group C, by 1.80.

For loading combinations consisting only of loads expected to act with their full value during the entire lifetime of the structure, both the strength and the stiffness values must be multiplied by 0.7.

In a continuous glued joint between a plate (board) flange and a maximum 30 mm wide web, the value for plate shear can be doubled. It is assumed that the distance from web to edge of plate is minimum 30 mm (measured perpendicular to the longitudinal direction of the joint), that the free distance between parallel joints is minimum 60 mm, and that the joint is not subjected to tension perpendicular to the plane of the joint.



Addendum 3.1

Canadian Exterior Douglas Fir Plywood. *)

a. Application.

Canadian Exterior Douglas Fir Plywood, manufactured and marked according to Canadian Standard CSA 0121, can be used in climate classes 1a, 1b, 2 and 3, assuming that the boards are suitably protected against climatic action (inclusive of rot) and that they are not used where they are likely to be directly exposed to water for a long period of time.

b. Strength and stiffness.

For loading category A and climate class 1b, the strengths and stiffnesses specified in the tables can be used.

Note:

For the present is used strength values corresponding to the statements in British Standard CP 112: 1967.

For loading category B, the strength values can be multiplied by 1.20, and for loading category C by 1.40.

For loading combinations consisting only of loads expected to act with their full value during the entire lifetime of the structure, both the strength and the stiffness values must be multiplied by 0.9.

For climate class 1a, all values can be increased by 10%.

For climate classes 2 and 3, the strength values for compression, bending and shear, and the stiffness figures must be multiplied by the factor 0.7, while the strengths for tension must be multiplied by 0.9.

The following notation is used in the table:

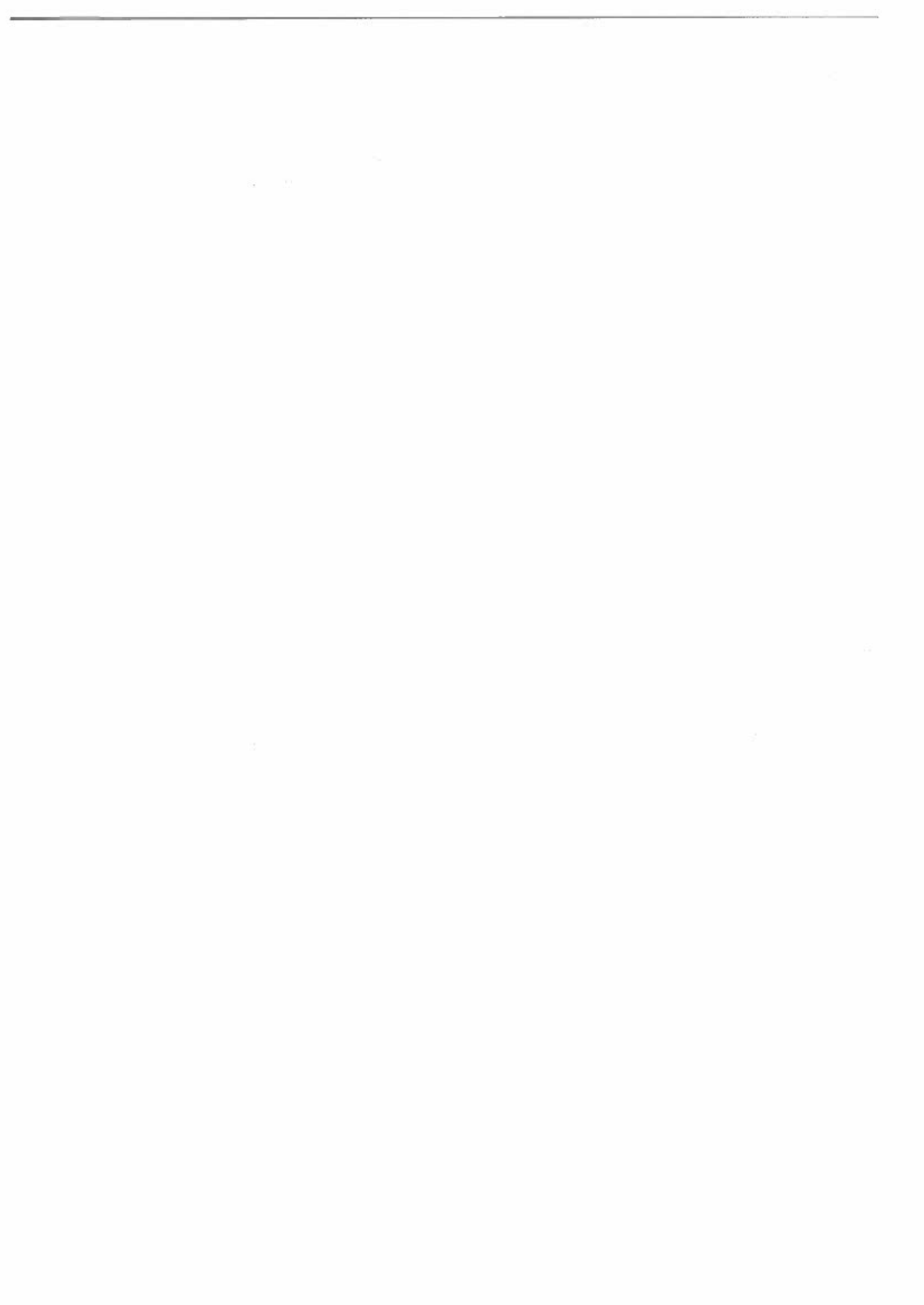
*) Corresponding adenda has been prepared for other plywood qualities (American, Swedish and British).

- m_0 Bending moment per unit length when the moment vector is perpendicular to the fibre direction in the outer plies (stresses in this fibre direction).
- m_{45} Bending moment per unit length when the moment vector forms an angle of 45° with the direction of the fibres.
- m_{90} Bending moment per unit length when the moment vector is parallel to the fibre direction in the outer plies.
- $(EI)_0$, $(EI)_{45}$ and $(EI)_{90}$: Bending stiffness per unit length, corresponding to the moments m_0 , m_{45} and m_{90} .
- n_0 Tensile force per unit length in tension along the fibre direction of the outer plies.
- n_{45} Tensile force per unit length in tension at an angle of 45° with the fibre direction of the outer plies.
- n_{90} Tensile force per unit length perpendicular to the fibre direction in the outer plies.
- n'_0 , n'_{45} and n'_{90} are analogous to n_0 , n_{45} and n_{90} , but for compression.
- $(ED)_0$, $(ED)_{45}$ and $(ED)_{90}$: Stiffness per unit length corresponding to the forces $n_0(n'_0)$, $n_{45}(n'_{45})$ and $n_{90}(n'_{90})$.
- s'_{90} Compressive strength perpendicular to the surface of the board.
- t_0 Shear stress corresponding to diaphragm effect (shear through the the thickness) in directions parallel with and perpendicular to the fibre directions.
- t_{45} Shear stress corresponding to diaphragm effect (shear through the thickness) in directions forming an angle 45° with the fibre directions.

t_{90} Shear stress where one of the shear stresses is perpendicular to the plane of the board (rolling shear).

G_0, G_{45} : Shear moduli corresponding to shear stresses t_0 and t_{45} .

In order to avoid errors at the present stage, thoroughly checked Danish tables are reproduced below (in the following), giving nominal, not characteristic, values for strength calculations. The characteristic values are obtained by multiplying the table values by 1.3.



Structural Research Laboratory
 Technical University of Denmark, DK-2800 Lyngby

RAPPORTER (Reports)

(1970 -

- | | | |
|-------|--|---------------------|
| R 11. | Bræstrup, Mikael W.: The Cosserat Surface and Shell Theory. 1970. | Out of print |
| R 12. | Askegaard, Vagn: Anvendelse af modelanalyse. 1970. | |
| R 13. | Solnes, Julius: The Spectral Character of Earthquake Motions. 1970. | Out of print |
| R 14. | Bræstrup, Mikael W.: Yield Lines in Discs, Plates and Shells. 1970. | Out of print |
| R 15. | Møllmann, J.: Beregning af hængekonstruktioner ved hjælp af deformationsmetoden. 1970. | Out of print |
| R 16. | Byskov, Esben: The calculation of Stress Intensity Factors Using the Finite Element Method with Cracked Elements. 1970. | |
| R 17. | Askegaard, V.: Grundlaget for adhæsion. 1970. | |
| R 18. | Summaries of Lecture Notes on Experimental Stress Analysis. 1970. | Out of print |
| R 19. | Sørensen, Hans Christian: Forskydning i jernbetonbjælker. 1970. | |
| R 20. | Sørensen, Hans Christian: Forskydningsforsøg med 12 jernbetonbjælker med T-tværsnit. 1971. | |
| R 21. | Møllmann, H.: Analysis of Hanging Roofs Using the Displacement Method. 1971. | Out of print |
| R 22. | Haurbæk, Poul E.: Dæmpede svingninger i spændbetonbjælker. Svingsningsforsøg med simpelt understøttede bjælker. | Publication pending |
| R 23. | Bræstrup, M.W.: Yield-line Theory and Limit Analysis of Plates and Slabs. 1971. | |
| R 24. | Dyrbye, Claës: Pendulum Vibration. 1971. | Out of print |
| R 25. | Møllmann, H.: Analytical Solution for a Cable Net over a Rectangular Plan. 1971. | |
| R 26. | Nielsen, J.: Silotryk. 1972. | Out of print |
| R 27. | Askegaard, V., M. Bergholdt and J. Nielsen: Problems in connection with pressure cell measurements in silos. 1972. | |
| R 28. | Ramirez, H. Daniel: Buckling of plates by the Ritz methods using piecewise-defined functions. 1972. | |
| R 29. | Thomsen, Kjeld & Henning Agerskov: Behaviour of butt plate joints in rolled beams assembled with prestressed high tensile bolts. 1972. | |
| R 30. | Julius Solnes and Ragnar Sigbjörnsson: Structural response to stochastic wind loading. 1972. | |
| R 31. | H. J. Larsen og H. Riberholt: Forsøg med uklassificeret konstruktionstræ. 1972. | |

